

Review

# Renewable Resource Biosorbents for Pollutant Removal from Aqueous Effluents in Column Mode

Lavinia Tofan <sup>1</sup> and Daniela Suteu <sup>2,\*</sup>

<sup>1</sup> Department of Environmental Engineering and Management, “Cristofor Simionescu” Faculty of Chemical Engineering and Environmental Protection, “Gheorghe Asachi” Technical University of Iasi, 700050 Iasi, Romania

<sup>2</sup> Department of Organic, Biochemical and Food Engineering, “Cristofor Simionescu” Faculty of Chemical Engineering and Environmental Protection, “Gheorghe Asachi” Technical University of Iasi, 700050 Iasi, Romania

\* Correspondence: danasuteu67@yahoo.com

**Abstract:** The present work deals with the continuous flow systems based on renewable resource biosorbents towards the green removal of various categories of chemical pollutants from aqueous media. The opening discussions are focused on: (a) renewable resources; (b) biosorbents based on renewable resources; (c) dynamic biosorption. After these, the renewable resources biosorbents are reviewed according to the parameters of breakthrough curves. Subsequently, the targeted biosorbents are systematized and analyzed according to the following criteria: (a) their ability to work as remediation agents for heavy metal ions and dyes, respectively; (b) their relevancy for continuous biosorption processes applied both to synthetic aqueous solutions and real wastewaters. The perspective directions of research for the implementation of biosorbents from renewable resources in practical column strategies for wastewater treatment are recommended.

**Keywords:** biosorption; column; heavy metals; dyes; renewable resource; wastewater treatment



**Citation:** Tofan, L.; Suteu, D.

Renewable Resource Biosorbents for Pollutant Removal from Aqueous Effluents in Column Mode.

*Separations* **2023**, *10*, 143. <https://doi.org/10.3390/separations10020143>

Academic Editor: Mohammed J. K. Bashir

Received: 2 February 2023

Revised: 15 February 2023

Accepted: 17 February 2023

Published: 19 February 2023



**Copyright:** © 2023 by the authors. Licensee MDPI, Basel, Switzerland. This article is an open access article distributed under the terms and conditions of the Creative Commons Attribution (CC BY) license (<https://creativecommons.org/licenses/by/4.0/>).

## 1. Introduction

In the conditions of raw material crisis and the need to find new structures biocompatible with the human body, renewable resources have proven to be particularly useful. The main targeted fields are the biosynthesis processes and the development of biomaterials with multiple applications in industry, medicine, and agriculture. The bio-based polymers originating from renewable resources are remarkable in recycling capacity, biodegradability, and long-term availability. At their center are the polysaccharides that comprise cellulose, lignin, chitin and chitosan, pullulan, starch, dextran, agarose, and alginic acids [1–3].

The accelerated development of life has led to the considerable reduction of natural water resources, which is why attention is focused on the application of different methods for purifying the ever-increasing amounts of wastewater, be it industrial, agricultural, or domestic. The wastewaters are loaded with variable amounts of countless pollutants of the most diverse forms and origins: inorganic (metal ions, anions), organic (solvents, pesticides, dyes, herbicides, fertilizers, drugs), biological or microbiological (phytotoxins, microorganisms, biological wastes). Their removal is a mandatory requirement imposed by the need to ensure the quality conditions imposed on drinking water. Numerous methods have been used over time for water depollution: extraction techniques, adsorption, flocculation, chemical precipitation, membrane processes, sonolysis, etc. [1–6]. The selection of the wastewater treatment methods is made based on economic and performance criteria, such as: pollutant type, practical implementation conditions, cost-benefit balance, ensuring the highest possible removal efficiency, the production of as low as possible waste quantities to avoid complicated and expensive subsequent techniques for their destruction.

Among the above-mentioned methods, the leader position is occupied by adsorption, with distinctive advantages: ease of application, flexibility, versatility, and a wide range of materials with adsorptive properties usable for both chemical and biological pollutants removal [7–14]. The cleaner alternative of adsorption, namely the biosorption consisting of the transfer of soluble substances from an aqueous medium to the surface of bio-based materials known as biosorbents, is also very challenging [15–19]. Biosorption can be regarded as a separation method that is performed by means of extracellular and intracellular bonds. These interactions are dependent on the nature of chemical species, biosorptive material structure, microbial metabolism, and transport process [20–22]. Similar to the biodegradation of organic compounds, biosorption involves the breaking and formation of chemical bonds that alter the molecular structure of the pollutant. This leads to changes in the solubility, adsorption characteristics, transport, and toxicity of metals or radionuclides. Biosorption by biosorbents for the removal of toxic metals and recovery of valuable metals [23–36] or for the retention of organic pollutant species (dyes, phenolic compounds, drugs) from aqueous media [35–51] is an effervescent area of research. By revision Scopus database, a search for the keyword “biosorbents” revealed 1559 studies published over 2018–2022, including 77.293% research articles, 10.712% review articles, 7.184% conference papers, and 3.85% book chapters.

Due to the constant expansion of both materials acting as biosorbents and the types of pollutants to be removed, it is obvious that biosorption remains an open topic. However, the large majority of the research has been performed on synthetic aqueous solutions at lab-scale batch systems. The information obtained from these studies is not sufficient to provide the data required for designing a wastewater treatment system for continuous operation. Therefore, the focus should be on the works on continuous biosorption processes that are not as popular as the batch ones. The studies on the continuous systems of biosorption have been critically analyzed to date in one single review article [52]. Even this article is not completely devoted to dynamic biosorption since, in an attempt to make a comparison between biosorption operation modes, it also addresses issues related to batch biosorption. Furthermore, it is restricted to the fixed bed column biosorption of pollutants, especially metals, from synthetic aqueous solutions.

In light of the above, the present article is intended to be a valuable guide for biosorption transposition to an industrial scale and its applicability to real systems. Thus, this article systematizes and interprets the significant results of research targeting continuous flow systems based on renewable resource biosorbents for pollutant removal. It is divided into three main parts, pointing out the renewable resources, the biosorbents derived from them, and the removal performances of the proposed biosorbents in dynamic systems of biosorption, respectively. The knowledge gained on the removal of metals and organic pollutants from synthetic and real wastewaters via continuous biosorption is, for the first time, brought together by this work.

## 2. Renewable Resources (Cellulose, Lignin, Chitin, Chitosan)

The most abundant renewable resource of natural polymers, but also the most representative natural polysaccharide, is undoubtedly *cellulose* [53]. Due to the fibrous structure (determined by the size and distribution of pores), high hygroscopicity (correlated with porous structure and presence of hydroxyl groups), and the possibility of functionalization with organic reagents, nowadays cellulose finds numerous applications in ever wider fields [54–57]. In its different utilization forms, *cellulose* is characterized by: (i) availability at low cost; (ii) spherical shape of particles; (iii) possibility of particle size selection; (iv) mechanical strength; (v) high porosity; (vi) wettability; (vii) compatibility with biological structures; (viii) rapid kinetics; (ix) functionalization susceptibility; (x) possibility of processing in different forms; (xi) high specific surface area; (xii) easiness of physical and chemical regeneration; (xiii) tolerance to biological structures; (xiv) relatively fast adsorption [57–59]. All these properties, its high abundance in nature, as well as its renewable character make cellulose an inexhaustible source as a raw material to make not only paper

and fibers but also a series of biocompatible products for the environment. Depending on the technological process used for their manufacture, cellulose-based materials can be created in several forms and types, ranging from granules, fibers, and microcrystalline powders to softwood pulp and bacterial cellulose.

*Chitin* belongs to the polyamino saccharides class of animal or vegetable origin, being the main constituent of the shell of crustaceans and of the hard integument of worms [60]. It is also part of the composition of some mushrooms and yeasts such as *Chytridiaceae*, *Blastocladiaceae* și *Ascomydes*. The mycelium of some species of *Penicillium* can contain up to 20% chitin. *Aspergillus niger* also represents an important source of chitin [61,62].

*Chitosan* is a linear polysaccharide of glucosamine and N-acetyl glucosamine, being composed of repeating units of 2-amino-2-deoxy-D-glucopyranose joined by  $\beta$ -D-1 $\rightarrow$ 4 linkages and a smaller number of N-acetyl-D-glucosamine (the deacetylated derivative of chitin). It is also an important component of the cell wall in various stages of the life cycle of some fungal species [60,63,64]. It is obtained from chitin through chemical or enzymatic hydrolysis of  $\alpha$ -chitin N-partially deacetylated using alkaline solutions (40–50%), at 100–160 °C, for several hours, in a proportion of around 50% [65]. Chitosan structure and properties depend on the chitin deacetylation degree. It is of the most promising materials which can also be used as an efficient biosorbent for the retention of different chemical pollutants.

### 3. Biosorbents Based on Renewable Resources

The use of conventional materials based on synthetic polymers or obtained by chemical synthesis has many disadvantages, such as the high cost, difficulty of the synthesis technologies, and the pollution generated by these. The need to eliminate these disadvantages and the current tendency to replace “chemical” products with natural products, “green” or “environmentally friendly”, existing in abundance in nature (such as those resulting as waste from agriculture or various industrial sectors) represented a favorable moment for a new type of adsorbent material implementation. These new adsorptive materials are represented by biosorbents that are generated by the processing of renewable resources (i.e., cellulose, lignocellulose, chitin, chitosan, vegetable waste, and algae).

In the last decades, the field of green materials has registered an accelerated development, both concerning the design and in the area of production and use of an ever-wider range of materials resulting from the processing of renewable resources. Their novelty and diversity come from nature, structure, and specific properties but also from the processing method type tailored to the intended applications. These applications are expanding more and more and are based both on the use of techniques for valorizing resources represented by industrial by-products or on innovative approaches (derivatizations, the creation of multi-component assemblies and supramolecular architectures, hybridizations, post-processing in different commercial forms, etc.) on already known materials [66].

An extremely wide spectrum of materials can be used as materials with chemical species retention properties, respectively:

- *Biomass* that encompasses: phytobiomass (lignocellulosic biomass from woody plants, peat); aquatic biomass; biomass from agricultural wastes, household biomass used in biogas production technologies; microbial biomass resulting from food or pharmaceutical industry [20,21,24,30,33,35,44,51,67–71];
- *Physicochemical-modified biomass* for the adsorption capacity improvement [72–75];
- *Immobilized biomass* is the result of biomass conversion into an easier-to-use form that ultimately contributes to the increase in the process efficiency of separation of pollutant-laden biomass from solution. Biomass immobilization can be carried out on different kinds of supports, with various shapes and porosities [76–78]. Immobilized biomass is promising as filling material in columns/bioreactors used in wastewater treatment.

Biosorbents are efficient for the removal of metallic ions from aqueous solutions in the presence of organic compounds or dissolved salts that are considered poisons for

ion exchange resins. Biosorbents can be used in the complete treatment of wastes or by coupling with another material, such as activated carbon, in treatments of chemical textile finishing. These materials have superior sorptive properties compared to conventional ones, with particular applicability in the final treatment of effluents.

### 3.1. Biosorbents Based on Cellulose

Among the renewable resources, available in large amounts and processed with low costs, that are addressed in view of testing their adsorptive properties for use as biosorbents in the treatment of wastewaters, the leader role is played by cellulose. This one can be used in many forms and types, ranging from fibers, microcrystalline powders, softwood pulp, and bacterial cellulose to production wastes and lignocellulosic (agro-industrial) wastes [20,32,66,70,72,79–84]. Lignocellulosic biomass provides large amounts of complex biopolymers containing mainly cellulose, hemicellulose, and lignin that are used to obtain nanocellulose [83,85].

In order to increase its efficiency as a biosorbent, the cellulose macromolecule is amenable to numerous relatively inexpensive processes of structural modification, such as the selective oxidations [66,72,86] cross-linking with different agents (acrylonitrile, hydroxylamine, acrylic acid, glycidyl methacrylate, urea) [72] or modifications with chemical reagents through esterification, halogenation, etherification methods [72,75]. New materials with higher specific surface area and porosity and reactive functional groups capable of interacting with polluting chemical species of organic or inorganic nature for their retention are obtained via these strategies.

### 3.2. Biosorbents Based on Chitosan

The second available biopolymer in nature, chitosan, has structural features due to which it shows distinctive chemical, mechanical, optical, and physical properties, high porosity, low density, regenerability, and biodegradability [60,87,88]. Apart from these, the processing easiness, non-toxicity, antibacterial properties, high reactivity, properties of coagulation, flocculation, and biosorption that are due to the presence of hydroxyl and amine-reactive groups in the macromolecular chains are also remarkable [61,87,89–92]. These characteristics make chitosan a potential alternative to its synthetic counterparts for environmental applications. Because of the presence of surface-active functional groups, it is possible to easily form bondings with various inorganic and organic substances, allowing its use as a biosorbent in various wastewater treatment processes [60,90,93–96]. However, some obvious disadvantages, such as the soft structure, high solubility in organic solvents, high percentage of swelling in water, low mechanical strength, and reduced surface, limit its use in industrial applications [97]. Furthermore, the chitin and chitosan processing under powder and flake forms results in a decrease in the adsorption capacity. The increase in adsorption capacity can be performed by its functionalization (grafting, coupling, and cross-linking) [98] or embedding in composite materials.

### 3.3. Biosorbents Based on Hydrogels

A relatively new and demanding category of biomaterials with adsorptive properties resulting from the processing of renewable resources is represented by *hydrogels*. These are three-dimensional matrices consisting of dense structures of natural and/or synthetic polymer networks that contain hydrophilic fractions and hydrophobic parts in different proportions, capable of absorbing large amounts of water or biological fluids [99–104]. The soft, rubbery consistency similar to living tissues makes them ideal materials for a variety of applications.

The hydrogels show a series of characteristic properties, such as the possibility of desired functionality achieving, reversibility, sterilization, and biocompatibility that fulfill both the requirements of materials used as biological biomaterials to treat or replace tissues and organs or the function of living tissues as well as to interact with the biological system [101,105–107]. Different polysaccharides or renewable resources can be used as

basic units subjected to the cross-linking process, the more well-known being cellulose, chitin, chitosan, polyvinyl acid, and pullulan [108–111].

Due to their particular characteristics, especially the capacity of swelling in water, high specific surface area, and the variety of surface functional active groups, the hydrogels have been proven to be very efficient as biosorbents used in water treatments.

#### 4. Dynamic Biosorption

The removal of pollutants from aqueous media via biosorption processes can be carried out in batch and dynamic systems. Distinguished by simplicity and the ability to work with small and constant volumes of solutions, the *biosorption batch mode* is the preferred option for lab-scale research. It is mainly focused on the study of the influence of the operating variables (pH, temperature, biosorbent dose, initial concentration of chemical species, contact time, agitation, biosorbent structure and size of its particles, structure of the targeted chemical species, size and shape of organic substance molecule or metal ion, electrical charge of chemical species, speciation of metal ions as function of pH values) on the biosorption processes [21]. The provided data serve as useful tools for: (i) setting the most suitable biosorption isotherm for process data modeling up to equilibrium and determination of the maximum capacity of the tested material; (ii) determination of the kinetic parameters and the corresponding kinetic model for rate controlling process step evaluation; (iii) calculation of thermodynamic parameters of the biosorption process in order to establish its spontaneity and thermic effect; (iv) identifying the most probable biosorption mechanism. Alternatively, *dynamic systems* are more complex and operate with variable and large volumes of solutions. They are of vital importance for the assessment of the biosorption process’s technical feasibility for applications to real-life samples.

##### 4.1. Continuous Flow Systems of Biosorption

Dynamic adsorption usually occurs in an open system in which the aqueous solution containing pollutant molecules or ions continuously flows through a column that uses a bed made of particles of adsorbent. The contact between the adsorbent bed and the liquid phase can be performed in at least four types of column systems that are briefly described in Figure 1: (i) fixed bed (up flow or down flow); (ii) moving bed; (iii) fluidized bed; (iv) pulsed bed.

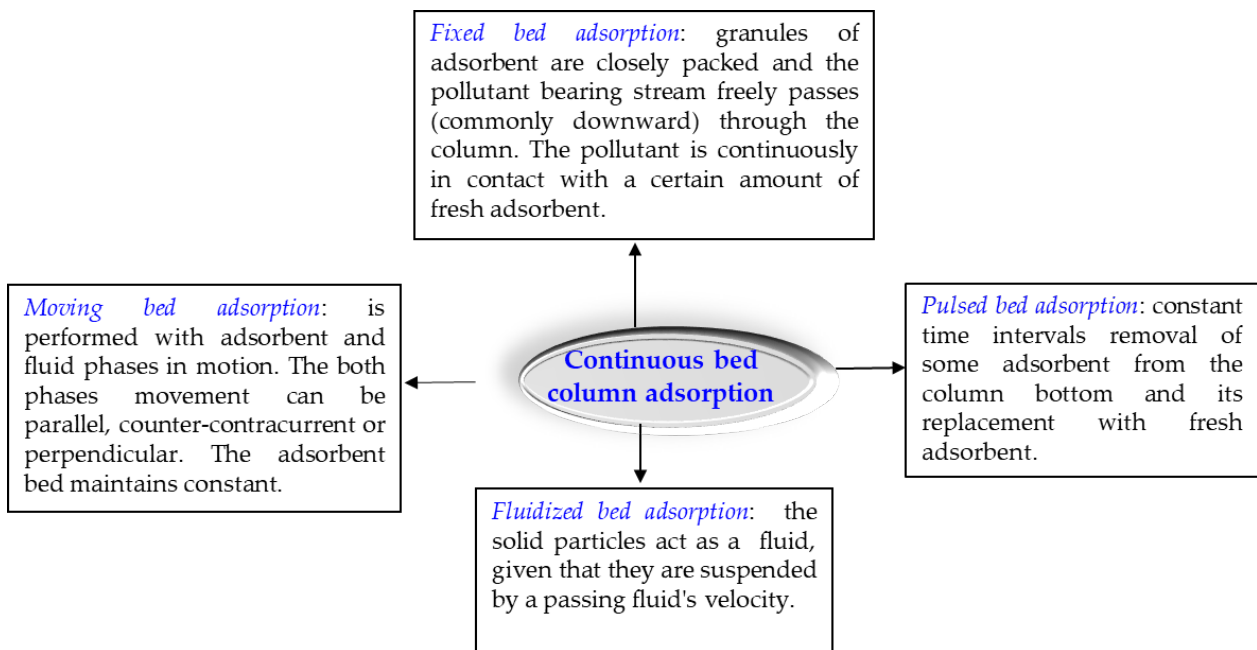


Figure 1. Main types of column adsorption procedures [9,112–114].

Choosing a working procedure in a dynamic regime from those in Figure 1 is made according to a set of criteria, including the nature of the adsorbent and the ratio between treatment efficiency and equipment operating costs. A literature scan has revealed that the continuous fixed and fluidized bed approaches fold the best on the requirements of the biosorption process. Of the above, the greatest attention is paid to the biosorption in fixed bed columns; the one in continuous fluidized beds is rarely addressed. As a proof of concept can be mentioned the biosorption of Pb(II), Cu(II), and Cd(II) ions from industrial wastewater using a fluidized bed of dry leaves of cabbage [115] and the continuous fluidized bed experiments on the removal of Cd(II) [116] and methylene blue dye [117] from aqueous solution using rice husk.

The prevalence of the continuous fixed bed columns over the other operating methods is due to its impressive number of benefits. Among these of special importance are:

- Operation and handling simpleness [118];
- Ensuring the highest possible gradient of concentration that is the process driving force [119];
- High operation yields [120];
- Increased efficiency in the use of biosorption capacity [121];
- Easiness in scaling up from lab-scale procedures [122];
- Quantitative removal of inorganic and organic species from high volumes of aqueous samples with a high level of contaminants by means of a known amount of biosorbent [51];
- Possibility of biosorbent reuse and recovery of valuable components [123];
- Potential for the automatization of the process stages [118,119].

In addition, the data obtained by using fixed bed columns are very useful for the decryption of the mechanism of adsorption that depends on a multitude of phenomena, such as: axial dispersion, fluid diffusion resistance, intraparticle diffusion resistance (pore and surface diffusion resistance) and equilibrium of adsorption [124,125].

#### 4.2. Breakthrough Curves

The effectiveness of the fixed-bed column is assessed by means of breakthrough curves, around which all dynamic studies of biosorption gravitate. These curves are given by the plots of the chemical species concentration or the normalized concentration of the chemical species in the effluent as a function of time or treated solution volume. The typical shape of a breakthrough curve that is a compelling source of information on the nature of the investigated biosorption process and on the pollutant's loading behavior in a continuous column is shown in Figure 2. The process parameters with the strongest influence on the steepness of the breakthrough curves are the height of the biosorbent bed ( $h$ ), volumetric flow rate ( $F_v$ ), and the initial concentration of the pollutant in the feed solution ( $C_0$ ).

The breakthrough curves are characterized by various derived parameters that are very heterogeneously addressed in the fixed bed column biosorption studies. The most representative and frequently reported breakthrough parameters are concisely described in Figure 3. Thus, on the basis of the parameters of breakthrough curves shown in Figure 3, suitable biosorbents for continuous fixed bed column processes are considered those that are distinguished by a long time of breakthrough, shorter time of saturation, and smaller mass transfer zone [9,18]. In view of these aspects, Table 1 systematizes the values of breakthrough curve parameters for the continuous fixed column biosorption of some inorganic and organic pollutant species from synthetic aqueous solutions on renewable resource biosorbents. The interesting data from Table 1 provide conclusive evidence for the implementation of the corresponding biosorbents in practical continuous flow systems for the biosorptive removal of pollutants from real industrial effluents.

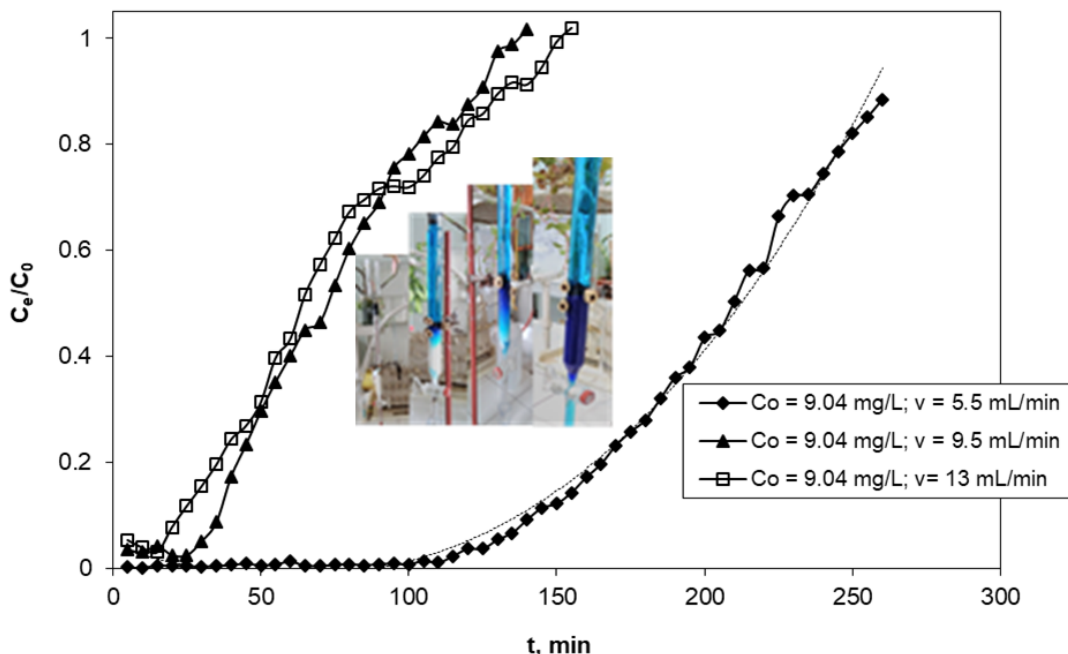


Figure 2. Breakthrough curve of Methylene Blue dye biosorption in a fixed-bed column filled with granulated *Cellets 200* cellulose. Operating conditions: T = 20 °C, C<sub>0</sub> = 9.04 mg/L.

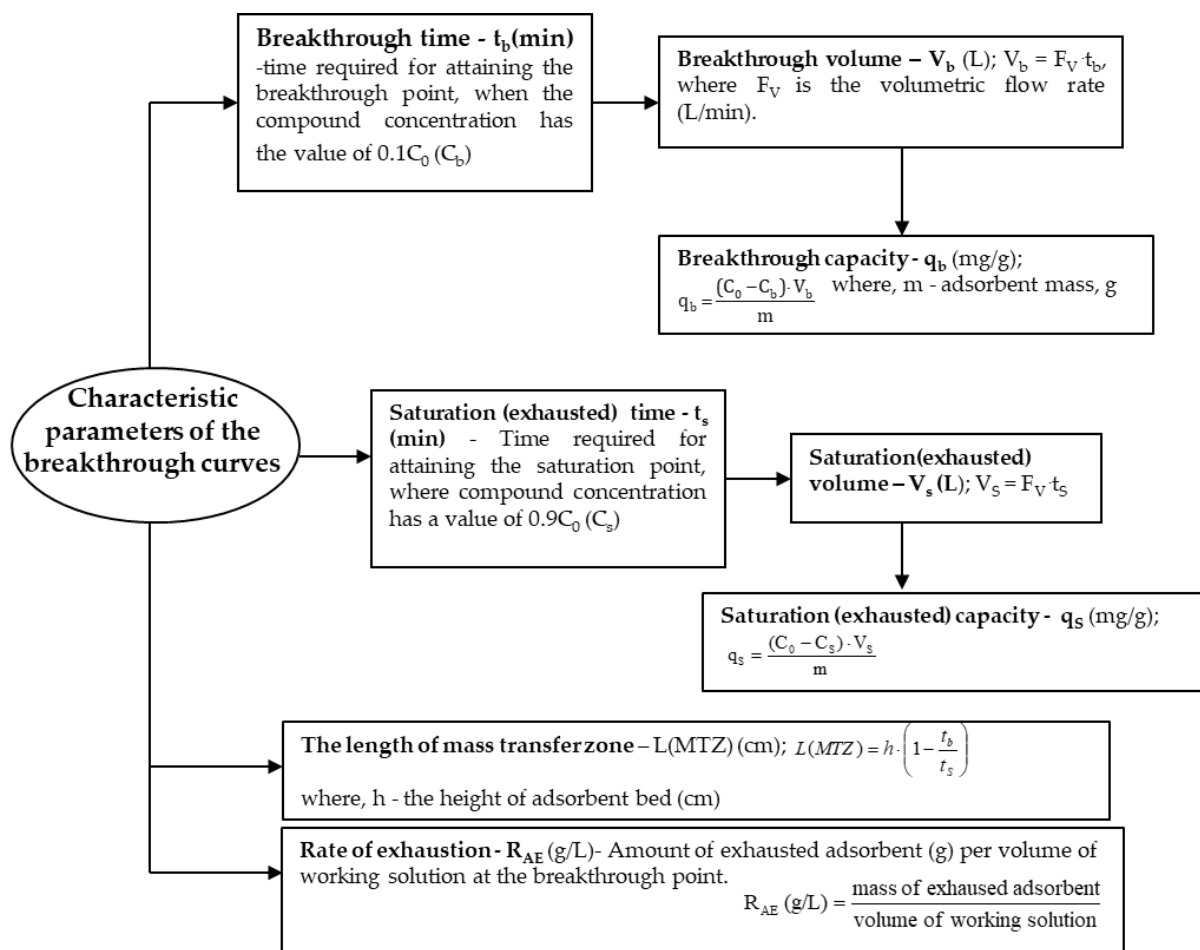


Figure 3. Characteristic parameters of the breakthrough curves [59,126,127].

**Table 1.** Characterization of dynamic biosorption systems for inorganic and organic pollutant removal via the parameters of breakthrough curves.

Chemical Pollutant	Biosorbent/ Experimental Conditions	Breakthrough Parameters	Remarks	Ref
Pb(II)/	Residue of allspice ( <i>Pimenta dioica</i> L. Merrill)/ C <sub>0</sub> = 15 mg/L; Fw = 20 mL/min; bed height = 15 cm	t <sub>b</sub> = 272 min; q <sub>b</sub> = 13.1 mg/g; t <sub>s</sub> = 339 min; q <sub>s</sub> = 16.2 mg/g; MTZ = 2.9 cm	Removal percentage of 99.7% for a treated volume of 6770 mL	[128]
Ni(II)/	Sugarcane bagasse/ C <sub>0</sub> = 100 ppm; Fw = 5 mL/min; bed height = 10 cm	t <sub>b</sub> = 1500 min; t <sub>s</sub> = 5750 min; MTZ = 4250 min; length of unused bed = 5.38 cm	Ni(II) uptake: 2.98 mg/g; mass of adsorbate treated: 1750 mg	[129]
Cd(II); Cu(II); Pb(II)/	Spent coffee ground; C <sub>0</sub> = 0.1 mM; Fw = 5.5 mL/min; bed height = 14 cm	t <sub>b</sub> = 50 min(Cd); 160 min(Cu); 220 min(Pb) q <sub>b</sub> = 0.0373 mmol/g(Cd); 0.0838 mmol/g(Cu); 0.135 mmol/g (Pb)	Reduced efficiency at low flow rate due to a significant axial dispersion phenomenon	[130]
Cr(VI)/	Modified corn stalk/ C <sub>0</sub> = 200 mg/L; Fw = 10 mL/min; bed height = 1.4 cm	t <sub>s</sub> = 288 min; empty bed contact time: 1.1 min; maximum capacity of column: 135 mg/g	Removal percent of 93.78% for a volume of effluent of 2880 mL	[131]
Mn(II); Cr ions/	Cashew nutshell activated with H <sub>2</sub> SO <sub>4</sub> / C <sub>0</sub> = 20.36 mg/L (Mn), 21.05 mg/L(Cr); Fw = 5 mL/min; bed height = 10 cm	t <sub>b</sub> = 600 min (Mn); t <sub>s</sub> = 1080 min (Cr); maximum capacity of column: 9.82 mg/g (Mn), 10.79 mg/g (Cr)	Removal percentage: 53.09% (Mn), 56.40% (Cr); volume of effluent = 6000 mL	[132]
Cr(VI)/	Activated neem bark/ C <sub>0</sub> = 50 mg/L; Fw = 10 mL/min mass of biosorbent = 175 cm	t <sub>b</sub> = 111.6 h; q <sub>s</sub> = 28.89 mg/g; empty bed residence time: 35.48 s; rate of exhaustion: 2.61 g/L	Removal percentage: 35.48%; amount of total Cr(VI) passed through column: 6.954 mg	[133]
Pb(II), Cd(II), Zn(II)/	Protonated citrus peels/ C <sub>0</sub> = 0.1 meq/L; Fw = 0.9 mL/min; bed height = 24 cm	t <sub>b</sub> = 50 h(Pb), 37 h(Cd), 30 h(Zn); q <sub>b</sub> = 57 mg/g(Pb), 22 mg/g(Cd), 11 mg/g(Zn); t <sub>s</sub> = 120 h(Pb and Cd), 110 h(Zn); q <sub>s</sub> = 85 mg/g(Pb), 44 mg/g (Cd), 20 mg/g(Zn)	Uptake order at breakthrough and saturation: Zn < Cd < Pb; concentration factors ranging from 34 to 129	[134]
Cu(II), Co(II)/	Oxidized sugarcane bagasse/C <sub>0</sub> = 1.26 mmol/L(Cu); 0.68 mmol/L(Co); bed height = 3.80 cm; pH = 5.5	q <sub>s</sub> = 0.554 mmol/g (Cu), 0.224 mmol/g (Co); height of the used bed: 1.58 cm (Cu), 0.68 cm (Co)	Values of biosorption capacity are 2.9% Cu) and 65.2% (Co) lower than those corresponding to batch systems	[135]
Ni(II)/	Base treated cogon grass ( <i>Imperata cylindrica</i> )/C <sub>0</sub> = 10 mg/L; Fw = 9.76 mL/min; bed height = 5.2 cm; pH = 5	t <sub>b</sub> = 18.1 min; V <sub>b</sub> = 180 mL; q <sub>b</sub> = 1.77 mg/g; t <sub>s</sub> = 96.7 min; V <sub>s</sub> = 952.6 mL; maximum capacity of column = 5.25 mg/g	Total effluent volume: 943.8 mL	[136]
Pb(II)/	Activated tea waste/ C <sub>0</sub> = 5 mg/L; Fw = 10 mL/min; bed height = 0.4 m	t <sub>b</sub> = 133 min; t <sub>s</sub> = 567 min; V <sub>s</sub> = 5700 mL; MTZ = 30.5 cm; maximum column capacity: 1.587 mg/g	Removal percentage of 52.8%; volume of effluent: 5.7 L	[137]
Pb(II)/	Binary adsorbent constituting of 75 wt% eggshells with 25 wt% waste sugarcane bagasse /C <sub>0</sub> = 100 mg/L; Fw = 4 mL/min; bed height = 12 cm; pH = 5.5	t <sub>b</sub> = 2700 min; V <sub>b</sub> = 6960 mL; t <sub>s</sub> = 3336 min; q <sub>s</sub> = 29.98 mg/g; MTZ = 2.29 cm; rate of biosorbent exhaustion: 3.58	Total removal percentage: 91%; column efficiency: 81%	[138]
Fe(III), Mn(II)/	Crushed sea shell/ C <sub>0</sub> = 425.4 mg/L; Fw = 5 mL/min; biosorbent mass = 60 g; pH = 2.3	t <sub>b</sub> = 345 min (Fe), 120 min(Mn); q <sub>b</sub> = 12.2 mg/g(Fe), 0.9 mg/g(Mn); q <sub>s</sub> = 18.8 mg/g(Fe), 1.44 mg/g(Mn); rate of biosorbent exhaustion: 34.8 g/L(Fe), 95.2 g/L (Mn)	Metal removal: 67.3%(Fe), 57.5% (Mn); metal uptake: 139.1 mg/g (Fe); 57.5 mg/g (Mn)	[139]
Cr(VI), total chromium/	Hass avocado ( <i>Persea americana</i> Mill. var. Hass) shell/ C <sub>0</sub> = 200 mg/L; Fw = 0.75 mL/min; biosorbent mass = 2 g; pH = 1.5.	q <sub>b</sub> = 184.39 ± 0.72 mg/g (Cr(VI), 127.63 ± 0.63 mg/g (total chromium)	Breakthrough curve steepness for total chromium biosorption has been strongly dependent on the pH of the influent solution	[140]
Cd(II), Ni(II)/	Mollusk shells/ C <sub>0</sub> = 209 mg/L (Cd), 105 mg/L(Ni); Fw = 1.5 mL/min; bed height = 15 cm; pH = 7.7.	V <sub>s</sub> = 15 L(Cd), 12.9 L(Ni); empty bed contact time = 785 min	Removal efficiency: 47.9% (Cd), 42.7%(Ni); column biosorption capacity: 1.69 mg/g (Cd), 0.19 mg/g(Ni);	[141]

Table 1. Cont.

Chemical Pollutant	Biosorbent/ Experimental Conditions	Breakthrough Parameters	Remarks	Ref
Cu(II)/	Carboxyl-modified jute fiber; C <sub>0</sub> = 100 mg/L; Fw = 54.78 mL/min; bed height = 8 cm	t <sub>b</sub> = 11.71 min; empty bed contact time = 0.46 min; MTZ = 5.86 cm	Biosorption efficiency: 48.92 %; equilibrium biosorption capacity: 29.37 mg/g	[142]
Cu(II)/	Amino-functionalized ramie stalk; C <sub>0</sub> = 0.5 mmol/L; Fw = 5 mL/min; bed height = 10 cm	t <sub>b</sub> = 100 min; V <sub>b</sub> = 500 mL; q <sub>b</sub> = 0.472 mmol/g t <sub>s</sub> = 120 min; V <sub>s</sub> = 600 mL; q <sub>s</sub> = 0.495 mmol/g; MTZ = 1.667 cm	Removal efficiency: -at breakthrough point: 99.26%; -at saturation point: 99.27%	[143]
Pb(II)/	Watermelon rind; C <sub>0</sub> = 500 mg/L; Fw = 1 mL/min; bed height = 5 cm	t <sub>b</sub> = 75 min; t <sub>s</sub> = 125 min; total metal adsorbed = 45.3 mg	Total metal percentage removal: 72.5%	[144]
Cr (VI)/	<i>Hibiscus Cannabinus</i> kenaf; C <sub>0</sub> = 0.5 mg/L; Fw = 2 mL/min; bed height = 15 cm	V <sub>b</sub> = 45 mL; q <sub>b</sub> = 9.2 µg/g; empty bed contact time = 2.96 min	Total removal: 52%; equilibrium adsorption capacity: 21 µg/g	[145]
Methylene Blue (MB) dye	Agricultural biomass from the Moroccan Sahara (ABMS) = prickly pear waste; C <sub>0</sub> = 80 mg/L; Fw = 4 mL/min; bed height = 5 and 15 mm.	t <sub>b,min</sub> = 120 min (h = 5 cm) t <sub>b,max</sub> = 250 min (h = 15 cm) t <sub>s,min</sub> = 360 min (h = 5 cm) t <sub>s,max</sub> = 640 min (h = 15 cm)	q <sub>max</sub> = 30.15 mg /g (C <sub>0</sub> = 120 mg/L; Fw = 4 m L/min; h = 10 cm)	[146]
Methylene Blue (MB)	Rice husk (RH) and torrefied rice husk (TRH) <i>in the fixed-bed column:</i> C <sub>0,MB</sub> = 9 mg/L; Fw = 100 mL /min; bed height = 0.65 m	<b>RH:</b> t <sub>b</sub> = 4 min; t <sub>total</sub> = 180 min; <b>TRH:</b> t <sub>b</sub> = 16 min; t <sub>total</sub> = 180 min;	q = 1.54 mg/g, R% = 26; V <sub>total effluent</sub> = 18,000 cm <sup>3</sup> q = 3.04 mg/g; R% = 51; V <sub>total effluent</sub> = 18,000 cm <sup>3</sup>	[117]
Methylene Blue (MB)	Rice husk (RH) and torrefied rice husk (TRH) <i>inverse fluidized-bed column:</i> C <sub>0,MB</sub> = 6 mg/L; Fw = 283 and 306 cm <sup>3</sup> /min (to obtain two superficial velocities of 0.0026 and 0.0024 m/s); bed height = 0.15 and 0.65 m	<b>RH</b> (F <sub>w</sub> = 306 cm <sup>3</sup> /min; h = 0.15 m): t <sub>b</sub> = 2 min; t <sub>total</sub> = 95 min; <b>TRH</b> (F <sub>w</sub> = 283 cm <sup>3</sup> /min; h = 0.15 m): t <sub>b</sub> = 22 min; t <sub>total</sub> = 95 min;	q = 2.77 mg/g, R% = 32; V <sub>total effluent</sub> = 29092 cm <sup>3</sup> q = 6.82 mg/g, R% = 51; V <sub>total effluent</sub> = 26,854 cm <sup>3</sup>	[117]
Methylene Blue	Cellulose nanocrystal-alginate hydrogel beads in fixed bed columns/ fixed beds with reverse flow: C <sub>0</sub> = 50, 150 and 250 mg/L; Fw = 1.17, 2.34 and 4.40 mL/min; bed height = 22, 44 and 66 cm	t <sub>s</sub> = 291.08 min (F <sub>w</sub> = 4.17 mL/min; V <sub>t</sub> = 1214.71 mL; qt = 19.35 mg/g t <sub>total</sub> = 234 min R% = 7.61	q = 255.5 mg/g (initial dye concentration 250 mg/L; Fw = 4.40 mL/min; bed depth of 7.4 cm)	[147]
Congo red (CR)	Free and immobilized in polymeric matrix sodium silicate agricultural waste biomass of <i>Nelumbo nucifera</i> (lotus)-NNLP/Continuous- flow fixed-bed: C <sub>0</sub> = 15 mg/L, pH = 6, Fw = 1 mL/min, bed height =2.5 cm	<i>Free NNLP:</i> t <sub>b</sub> = 8.75 h; t <sub>s</sub> = 17.5 h; V <sub>effl.</sub> = 1.05 L; <i>Immobilized NNLP:</i> t <sub>b</sub> = 6.5 h; t <sub>s</sub> = 13.5 h; V <sub>effl.</sub> = 0.81 L;	Q = 3.236 mg/g (free NNLP); R% = 76.42 Q = 2.754 mg/g (immobilized NNLP); R% = 67.3	[148]
Reactive Black 5 (RB5) dye	Hydrogel chitosan (CH); chitosan covalently cross-linked with epichlorohydrin (CH-EECH); chitosan ionically cross-linked with sodium citrate (CH-CIT); dynamic (flow) in an unconventional air-lift type loop reactor; C <sub>0</sub> = 50 mg RB5/L; Fw= 0.1 V/h (V-volume of reactor).; <b>S1</b> = "monocomponent" solution (deionized water + RB5) with a C <sub>0, RB5</sub> = 50 mg/L	t <sub>b</sub> ( <b>CHs</b> ) = 44 h/S1 t <sub>s</sub> ( <b>CHs</b> ) =904 h/S1 t <sub>b</sub> ( <b>CHs-CIT</b> ) = 132 h/S1 t <sub>s</sub> ( <b>CHs-CIT</b> )= 920 h/S1 t <sub>b</sub> ( <b>CHs-ECH</b> ) = 348 h/S1 t <sub>s</sub> ( <b>CHs-ECH</b> ) = 964 h/S1	q <sub>0</sub> ( <b>CHs</b> ) = 1504.7 mg RB5/g q <sub>0</sub> ( <b>CHs-ECH</b> ) = 2777.3 mg RB5/g-S1 (Thomson model)	[149]
Red dye 40	Alginate-chitosan sulfate hydrogels/ fixed-bed columns; two columns of 13 and 33 cm of height and two Fw (20 and 40 mL/h); C <sub>0</sub> = 20 mg/L; pH = 5;	t <sub>b</sub> = 1.8 h (Fw = 20 mL/min; h = 33 cm) t <sub>final</sub> = 450 h	q = 128 mg/g	[150]

### 4.3. Modeling the Biosorption Process in Dynamic Regime

In order to obtain information of high practical value, such as biosorption capacity, service time, usable bed length, and rate constant, the breakthrough data are usually analyzed with the aid of models of fixed bed column dynamics. These models rely on non-linear isotherms and axial dispersion, intraparticle diffusion, and external film resistance hypotheses [9,10].

The models with extended applicability are the Thomas model, Yoon–Nelson model, Bohart–Adams model, bed depth service time (BDST) model, Clark model, Wolborska model, and the modified dose–response model. The notoriety of these models is due to the fact that their equations can be linearized, allowing assessment of the model parameters by analysis of linear regression [151,152]. A short description of these models is given in Table 2. Among the models in Table 2, the Thomas model is the most commonly used. Similar to the Langmuir maximum capacity of biosorption in batch systems, the dynamic capacity of biosorption provided by the Thomas model usually serves as a reference for biosorbent comparison in continuous flow studies.

**Table 2.** Models of continuous fixed bed biosorption [153–159].

Model	Linear Form with Variable/Linear Plot	Assumption
Thomas (TH)	$\ln\left(\frac{C_0}{C_t} - 1\right) = \frac{k_{TH} \cdot q_0 \cdot m}{F_w} - \frac{k_{TH} \cdot C_0 \cdot V_{eff}}{F_w} \quad (1)$ <p>where: <math>C_0</math> and <math>C_t</math>-the pollutant concentration at initial moment (<math>t = 0</math>) and time <math>t</math> (mg/L); <math>k_{TH}</math>-the Thomas constant (L/min mg); <math>F_w</math>-the volumetric flow rate (L/min); <math>q_0</math>-the maximum biosorptive capacity (mg/g), <math>m</math>-biosorbent mass (g) and <math>V_{eff}</math>-the treated volume at time <math>t</math> (L). Linear plot: <math>\ln[(C_0/C_t)-1]</math> versus <math>t</math>. Model parameters: <math>K_{TH}</math> and <math>q_0</math></p>	<p>-the biosorption equilibrium follows the Langmuir model; -the rate kinetics is governed by the second-order reversible equation</p>
Yoon–Nelson	$\ln\left(\frac{C_t}{C_0 - C_t}\right) = k_{YN} \cdot t - t_{1/2} \cdot k_{YN} \quad (2)$ <p>where: <math>k_{YN}</math>-the Yoon–Nelson rate constant (<math>\text{min}^{-1}</math>); <math>t_{1/2}</math>-the time required for 50% pollutant breakthrough; <math>t</math>-biosorption time (min). Linear plot: <math>\ln [C_t/(C_0-C_t)]</math> versus <math>t</math>. Model parameters: <math>k_{YN}</math> and <math>t_{1/2}</math></p>	<p>-the decreasing of the biosorption rate for each biosorbate molecule is proportional to the probability of biosorbate breakthrough onto biosorbent bed.</p>
Bohart–Adams	$\ln\left(\frac{C_0}{C_t} - 1\right) = k_{BA} \cdot q_0 \cdot \frac{h}{u} - k_{BA} \cdot C_t \cdot t \quad (3)$ <p>where: <math>k_{BA}</math> is the Bohart–Adams rate constant (<math>1/\text{min} \times \text{mg}</math>); <math>q_0</math> is the maximum biosorption capacity per unit volume of the biosorption column (mg/L); <math>u</math> is the linear velocity of the biosorbate solution (cm/min), and <math>h</math> is the bed height or depth (cm). Linear plot: <math>\ln[(C_t/C_0)-1]</math> versus <math>t</math> Model parameters: <math>k_{BA}</math> and <math>q_0</math></p>	<p>-the biosorption rate is proportional to the amount or concentration of biosorbate in the bulk liquid phase and to the residual absorption capacity of the biosorbent; -ignoring axial dispersion effects. -rectangular isotherm with quasi-chemical rate kinetics.</p>

Table 2. Cont.

Model	Linear Form with Variable/Linear Plot	Assumption
Bed Depth Service Time Model (BDSTM)	$t = \frac{q_0 \cdot h}{C_0 \cdot u} - \frac{1}{k_{BDST} \cdot C_0} \ln\left[\left(\frac{C_0}{C_t}\right) - 1\right] \quad (4)$ <p>where: <math>k_{BDST}</math> is the BDST rate constant (L/mg min); <math>q_0</math> is the maximum biosorption capacity per unit volume of the biosorption column (mg/L), <math>h</math> is the bed height or depth (cm) and <math>u</math> is the linear velocity of the biosorbate solution (cm/min) The linear plot: bed height (<math>h</math>) versus <math>q_0</math> Characteristic parameters: <math>k_{BDST}</math> and <math>t_{1/2}</math></p>	<p>-the existence of a linear relationship between column bed height and service time in terms of biosorbate concentration and biosorption parameters; -resistances provided by the liquid phase (external diffusion) and the solid particles (intraparticules) are insignificant; -chemisorption at the interface between the biosorbent and the biosorbate controls the majority of the biosorption kinetics.</p>
Clark (CM)	$\left(\frac{C_{in}^{n-1}}{1 + A \cdot e^{-r' \cdot t_b}}\right) 1/(n-1) = C \quad (5)$ $A = \left[\frac{C_{in}^{n-1}}{C_b^{n-1}}\right] \cdot e^{r' \cdot t_b} \quad (6)$ $r' = (n-1) \cdot \frac{K}{F_w} \cdot \frac{dz}{dt} \quad (7)$ <p>where: <math>C_{in}</math> and <math>C_b</math> are the inflow concentration of the biosorbate and breakthrough concentration (mg/L), <math>t_b</math> is the service time (min). Linear plot: <math>C_t/C_0</math> versus <math>t</math> Model parameters: <math>A</math> and <math>r'</math></p>	<p>-equilibrium isotherm fits to Freundlich model; -shape of MTZ is constant and the biosorption is completely achieved at the end of the column; -biosorbates behave on column like “a piston” -the continuity equation of mass is applicable for the liquid phase.</p>
Wolborska (WM)	$\ln\left(\frac{C_t}{C_0}\right) = \frac{\beta \cdot C_0 \cdot t}{q_0} - \frac{\beta \cdot h}{u} \quad (8)$ <p>where: <math>\beta</math> is the film diffusivity (cm<sup>2</sup>/s). Linear plot: <math>\ln(C_t/C_0)</math> versus <math>t</math> Model parameters: <math>\beta</math> and <math>q_0</math></p>	<p>-the concentration profile of the biosorbate moves in the axial direction with a consistent velocity; -the early region of the breakthrough curve is completely controlled by the film diffusional resistances with uniform kinetic coefficient values. -the width of breakthrough curve width and its steepness degree of steepness are almost consistent.</p>
Modified Dose Response (MDRM)	$\ln\left(\frac{C_t}{C_0 - C_t}\right) = a \cdot \ln(C_0 \cdot F_w) - a \cdot \ln(q_{mdr} \cdot m) \quad (9)$ <p>where: <math>a</math> is the model parameter and <math>q_{mdr}</math> is the biosorptive capacity defined by the modified dose response model Linear plot: <math>\ln\left(\frac{C_t}{C_0 - C_t}\right)</math> versus <math>\ln(C_0 \cdot F_w)</math> Model parameters: <math>a</math> and <math>q_{mdr}</math></p>	

However, due to their empirical or semi-empirical nature, the models in Table 2 are unable to supply detailed information on the design parameters [160,161]. An efficient solution to this problem can be represented by successful computer simulations.

### 5. Overview of the Biosorbents Targeted in Continuous Biosorption Studies for the Removal of Pollutant Chemical Species from Synthetic Solutions and Real Wastewater

Despite their significance for industrial practicability, especially in the context of sustainable and circular economy, the continuous biosorption processes are not very popularly studied. The results of the relevant studies that describe the effective continuous biosorptive removal ability for heavy metal ions and dyes of biosorbents are displayed in Tables 3 and 4, respectively. In order to give a faithful picture through these tables, the behavior of renewable resource biosorbents in dynamic systems of biosorption is suggestively presented by means of the models that have been used for breakthrough curve modeling (Table 2), and their performances have been characterized mainly by the dynamic biosorption capacity.

**Table 3.** Renewable resource biosorbents for fixed bed column removal of heavy metals from synthetic solutions.

Targeted Metal Ion	Biosorbent	Working Conditions	Applied Breakthrough Models	Thomas Capacity of Biosorption	Refs.
Pb(II)	Sugarcane bagasse	Fw = 100 mL/min; bed height = 30 cm; C <sub>0</sub> = 20 mg/L Fw = 1.6 mL/min; bed height = 28 cm; C <sub>0</sub> = 10 mg/L; pH = 5 Fw = 2 mL/min; bed height = 3 cm; C <sub>0</sub> = 300 mg/L; pH = 5.4–5.7	Thomas	4.54 mg/g	[162]
Cu(II)			Bohart–Adams	3.98 mg/g	
Pb(II)			Yoon–Nelson	0.143 mg/g	
Cd(II)			Thomas	0.133 mg/g	
Cu(II)			Yoon–Nelson	22.2 mg/g	
Cd(II)			Dose–response	26.8 mg/g	
Ni(II)	Carboxylated sugarcane bagasse	Fw = 1.4 mL/min; bed height = 3.2 cm; C <sub>0</sub> = 0.95 mmol/L (Cu); 1.10 mmol/L (Co); 3.49 mmol/L (Ni)	Thomas	12.1 mg/g	[163]
Pb(II)			Thomas	31.8 mg/g	
Cu(II)			Bohart–Adams	0.98 mmol/g	
Co(II)	Rice straw	Fw = 10 mL/min; bed height = 10 cm; C <sub>0</sub> = 0.01 mmol/L	Thomas	1.06 mmol/g	[160]
Ni(II)			Bohart–Adams	0.76 mmol/g	
Cd(II)	Wheat straw ( <i>Triticum sativum</i> )	Fw = 10 mL/min; bed height = 10 cm; C <sub>0</sub> = 0.01 mmol/L	Yoon–Nelson	1.62 × 10 <sup>−3</sup> mmol/g	[165]
Pb(II)			Bed-Depth Service Time	1.70 × 10 <sup>−3</sup> mmol/g	
Cd(II)	Modified rice straw	Fw = 0.3–1 L/min; bed height = 0.5–2 m; C <sub>0</sub> = 100 mg/L	Dose–response	14.8 mg/g	[166]
Cd(II)			Thomas	43 mg/g	
Ni(II)	Grape stalk wastes	Fw = 1.071 mL/min; bed height = 2 cm; C <sub>0</sub> = 50 mg/g	Bohart–Adams	43 mg/g	[167]
Pb(II)			Yoon–Nelson	43.08 mg/g	
Cd(II)	Sesame waste	Fw = 11 mL/h; bed height = 2 cm; C <sub>0</sub> = 60 mg/L (Pb); 30 mg/g (Cd); particle size: 0.8–1 mm	Thomas	18.18 mg/g	[130]
Cd(II)			Bohart–Adams	22.88 mg/g	
Cr(VI)	Pistachio shell	Fw = 2.5 mL/min; bed height = 2 cm; C <sub>0</sub> = 60 mg/L; pH = 5.5	Yoon–Nelson	19.50 mg/g	[168]
Cr(VI)			Yan; Thomas	19.50 mg/g	
Total Cr	<i>Quercus crassipes</i> acorn shell	Fw = 10 mL/min; bed height = 5 cm; C <sub>0</sub> = 15 mg/L	Bohart–Adams	113.3 ± 3.75 mg/g	[169]
Total Cr			Yoon–Nelson	113.3 ± 3.75 mg/g	
Total Cr	<i>Quercus crassipes</i> acorn shell	Fw = 0.75 mL/min; bed height = 6.5 cm; C <sub>0</sub> = 200 mg/L; pH = 2	Yan; Thomas	113.3 ± 3.75 mg/g	[170]
Total Cr			Bohart–Adams	113.3 ± 3.75 mg/g	
Total Cr	<i>Quercus crassipes</i> acorn shell	Fw = 0.75 mL/min; bed height = 6.5 cm; C <sub>0</sub> = 200 mg/L; pH = 2	Dose–response	113.3 ± 3.75 mg/g	[170]
Total Cr			Yoon–Nelson	113.3 ± 3.75 mg/g	

Table 3. Cont.

Targeted Metal Ion	Biosorbent	Working Conditions	Applied Breakthrough Models	Thomas Capacity of Biosorption	Refs.
Pb(II) Cr(VI)	Rice husk	Fw = 30 mL/min; bed height = 10 cm; C <sub>0</sub> = 20 mg/L	Thomas Bohart–Adams Yoon–Nelson Wolborska	32.62 mg/g 11.04 mg/g	[171]
Cd(II)	Treated rice husk	Fw = 9 mL/min; bed height = 2.8 cm; C <sub>0</sub> = 20 mg/L	Thomas Bohart–Adams Yoon–Nelson	249 mg/g	[172]
Cd(II)	Orange peels	Fw = 2–15.5 mL/min; bed height = 24–75 cm; C <sub>0</sub> = 5–15 mg/L	Thomas Bohart–Adams Yoon–Nelson	0.40 mmol/g	[173]
Cu(II)	Coconut shell	Fw = 10 mL/min; bed height = 20 cm; C <sub>0</sub> = 10 mg/L	Thomas Bed-Depth Service Time Yoon–Nelson Clark	53.498 mg/g	[174]
Cr(VI)	Acid-activated water caltrop ( <i>Trapa natans</i> ) shell	Fw = 2 mL/min; bed height = 2 cm; C <sub>0</sub> = 50–150 mg/L	Thomas Bohart–Adams Yoon–Nelson Bed-Depth Service Time	55.44–129.02 mg/g	[175]
Cu(II)	Barley powder Alkalized roasted barley powder	Fw = 2.5 mL/min; biosorbent mass = 2 g; C <sub>0</sub> = 40–500 mg/L; pH = 5.5	Thomas Bed-Depth Service Time	23.2 mg/g 29.6 mg/g	[176]
Cd(II)	<i>Moringa oleifera</i> seed powder	Fw = 2 mL/min; biosorbent mass = 2 g; C <sub>0</sub> = 300 µg/L; pH = 7	Thomas	68.53 µg/g	[177]
Cr(VI)	Modified corn stalk	Fw = 5 mL/min; bed height = 1.4 cm C <sub>0</sub> = 200 mg/L; pH = 4.91	Thomas Bohart–Adams Yoon–Nelson	152.323 mg/g	[137]
Co(II) Pb(II)	<i>Ficus benghalensis</i> L. leaf powder	Fw = 1 mL/min; bed height = 2 cm; C <sub>0</sub> = 20 mg/L	Thomas Bohart–Adams Yoon–Nelson	10.85 mg/g 13.75 mg/g	[178]
Cr(VI)	<i>Psidium guajava</i> leaves	Fw = 40 mL/min; bed height = 10 cm; C <sub>0</sub> = 20 mg/L	Thomas Bohart–Adams	15.96 mg/g	[179]
Cu(II)	Kenaf fibers	Fw = 6 mL/min; bed height = 30 cm; C <sub>0</sub> = 100 mg/L	Thomas Bed-Depth Service Time	47.27 mg/g	[180]
Cd(II)	Date palm trunk fibers	Fw = 10 mL/min; bed mass = 4 g; C <sub>0</sub> = 110 mg/L	Thomas Yoon–Nelson Wolborska	20.93 mg/g	[181]
Cu(II) Co(II)	Crab shells	bed height = 25 cm	Thomas Bed-Depth Service Time	52.07 mg/g 20.47 mg/g	[182]
Cd(II)	Cockle shells ( <i>Anadara Granosa</i> )	Fw = 8 mL/min; bed mass = 5 g; bed height: 4.8 cm; C <sub>0</sub> = 200 mg/L	Thomas Bohart–Adams Yoon–Nelson	142.33 mg/g	[183]
Cd(II)	Freshwater mussel shells	Fw = 9 mL/min; bed height = 5 cm; C <sub>0</sub> = 10 mg/L	Thomas	7.86 mg/g	[184]

**Table 4.** Renewable resource biosorbents for dye removal from synthetic solutions by continuous biosorption processes.

Organic Chemical Pollutant	Biosorbent/ Experimental Conditions	Applied Model/Efficiency, [q (mg/g) /R%]	Ref.
Methylene Blue dye	agricultural biomass from the Moroccan Sahara-prickly pear waste/Fw = 2, 4, and 6 mL/min; bed height = 5, 10, and 15 mm; C <sub>0</sub> = 40, 80, 120 mg/L	response surface methodology based on the Box–Behnken design; Thomas; Yoon and Nelson q = 30.15 mg/g	[146]
Basic Violet 10 (BV10) and Direct Blue 151 (DB151)	pine bark-compost/Fw = 10–30 mL/min; bed height = 5.1–17.8 cm; C <sub>0</sub> = 50–150 mg/L; 25 °C; pH 3.0	BDST model, proposed by Bohart and Adams; Thomas model q = 112.6 for BV10 q = 34.7 mg/g for DB151	[185]
Crystal violet dye(CV)	agricultural wastes, <i>Citrullus lanatus rind</i> and <i>Cyperus rotundus</i> /Fw = 10–20 mL/min; bed height = 10–30 cm; C <sub>0</sub> = 10–25 mg/L	Bed Depth Service Time (BDST); Thomas; Yoon–Nelson q = 46.68 and 54.24 mg/g for CV in case of <i>Citrullus lanatus rind</i> and <i>Cyperus rotundus</i>	[186]
Reactive Orange 84 dye (RO84)	cotton flower agro-residue based activated carbon (CFAC)/Fw = 15 mL/min; bed height = 5 cm; C <sub>0</sub> = 200 mg/L	Thomas, Yoon Nelson and Bed Depth Service Time (BDST) models. q = 720 mg of RO84 per 4.67 g of CFAC adsorbent (154.175 mg/g)	[187]
Methylene Blue dye	melon peel/Fw = 0.6, 0.9 and 1.3 L/h; bed height = 10 cm; C <sub>0</sub> = 50 or 25 mg MB/L; 25 °C	Bohart and Adams, Clark, Wolborska, Yoon and Nelson models R(%)dyes = 60 to 76%	[188]
cationic dyes (meldola blue, methylene blue, chrysoidine G, crystal violet); anionic dyes (ethyl orange, metanil yellow, acid blue 113)	fertilizer plant waste carbon slurry/ Fw = 1.5 mL/min; C <sub>0</sub> = acid blue 113–5.0 × 10 <sup>−4</sup> M; metanil yellow, 6.0 × 10 <sup>−4</sup> M and ethyl orange, 6.0 × 10 <sup>−4</sup> M; adsorbent particles of size = 200–250/(50–200) mesh	R(%)phenols = 53–58% q = 217, 211, 104, 126, 233, 248, 267 mg/g for meldola blue, crystal violet, chrysoidine G, methylene blue, ethyl orange, metanil yellow, acid blue 113	[189]
phenol, 2-chlorophenol, 4-chlorophenol and 2,4-dichlorophenol)	Fertilizer plant waste carbon slurry/ Fw = 1.5 mL/min; C <sub>0</sub> : phenol = 6.0 × 10 <sup>−4</sup> M; chlorophenol = 6.0 × 10 <sup>−4</sup> M; 2,4-dichlorophenol = 1.0 × 10 <sup>−3</sup> M; adsorbent particles of size = 50 to 200; bed height = 3.1 cm; mass: 0.5 g	q = 25.6/72.2/82.2 and 197.3 mg/g for phenol/2-chlorophenol/4-chlorophenol and 2,4-dichlorophenol	[190]
Congo red dye	cellulose beads and cellulose-graphene nano-platelets beads/batch reactor; Fw = 0.01–0.04 L/min; bed height = 20 cm; C <sub>0</sub> = 15 mg/L; pH 7.0	q = 98.1 and 139.6 mg/g for cellulose and cellulose-GNP beads	[191]
Methylene Blue (MB) and Congo Red (CR) dyes	the Moroccan cypress cone <i>Cupressus Sempervirens</i> from Fez region (Morocco)/Fw = 2 mL/min; mass of biosorbent = 0.3/0.5 /0.7 g; C <sub>0</sub> = 50 mg/L; particles size = 200 μm	Thomas and Yoon–Nelson’s q = (79.21–336.82) mg/g-MB q = (72.12–325.18) mg/g-CR	[192]
Direct Blue 71 dye	chitosan–glutaraldehyde/ Fw = 1–3 mL/min; bed height = 3–12 cm; C <sub>0</sub> = 15–50 mg/L	Adams–Bohart, Thomas q = 343.59 mg/g (Fw = 1 mL/min; C <sub>0</sub> , Direct Blue 71 = 50 mg /L; bed height = 3 cm)	[193]

Table 4. Cont.

Organic Chemical Pollutant	Biosorbent/ Experimental Conditions	Applied Model/Efficiency, [q (mg/g) /R%]	Ref.
Methylene Blue dye	torrefied rice husk/ fixed-bed adsorption column: Fw = 100 and 150 mL/min; adsorption column with 20.83 g adsorbent; C <sub>0, MB</sub> = 6 and 9 mg/L. fluidized-bed bioadsorption column: Fw = 0.0026 and 0.0024 m/s; adsorption column with 25 g adsorbent; C <sub>0, MB</sub> = 6 and 9 mg/L.	in the fluidized-bed biosorption column R = 84%; q = 6.82 mg/q in the fixed-bed biosorption column R = 52%; q = 2.76 mg/g	[117]
Brilliant Black BN dye	chitosan beads impregnated with a cationic surfactant Cetyl Trimethyl Ammonium Bromide/Fw = 0.8 mL/min; bed height = 8 cm; C <sub>0</sub> = 100 ppm	Thomas Adams–Bohart; Yoon–Nelson q = 6.80 mg/g	[194]
Methylene Blue dye	cellulose nanocrystal-alginate hydrogel Fw= 4.40 mL/min; bed height = 22 cm; C <sub>0</sub> = 100, 250, 400 and 550 mg/L.	q = 255.5 mg/g	[147]
Methylene Blue dye	crab shell chitosan/neem leaf composite/Fw = 2.17 and 2.90 mL/min; bed height = 2.5 and 5.0 cm; C <sub>0</sub> = 50 and 200 mg/L	Thomas Adams–Bohart q = 77 mg/g	[195]
Suncion Red H_R (SRH-R) and Sunzol Blue RS (SB-RS)	eggshell powder–chitosan gel core-shell/Fw = 5, 8 and 11 mL/min; bed height =15 cm; C <sub>0</sub> = 25 and 50 mg/L	Clark; Adams–Bohart; Bed-Depth Service Time (BDST)	[196]
Drimarine Black CL-B dye	untreated, hydrochloric acid treated and immobilized peanut husk/ Fw = 1.8–5.4 mL/min; bed height = 1.5 to 3.5 cm; C <sub>0</sub> = 50–100 mg/L	Thomas; Bed Depth Service Time (BDST) q = 10.3–15.23 mg/g	[197]
Congo red (CR)	free and immobilized agricultural waste biomass of <i>Nelumbo nucifera</i> (lotus) in Calcium Alginate, Polyvinyl Alcohol, Polysulfone, Sodium Silicate/Fw = 1 mL/min; bed height = 2.5 cm; C <sub>0</sub> = 15 mg/L	Thomas;Yoon–Nelson; Adams–Bohart Bed Depth Service Time (BDST); Wolborska q = 3.236 mg/g (free biosorbent) q = 2.621 mg/g (Sodium silicate gel-immobilized NNLP adsorbent)	[148]
Methylene Blue (MB)	banana peels (BP)/Fw = 1 and 3 mL/min; C <sub>0</sub> = 100 and 200 mg/L; masses of adsorbent = 2.43, 4.86, 7.29 g	1-D advection–dispersion–sorption model coupled with the Langmuir kinetic model q = (0.19–0.222) kg/kg	[198]

As can be seen from Tables 3 and 4, the approaches to the behavior of biosorbents based on cellulose in continuous flow systems clearly surpass those related to those based on chitosan. The most targeted heavy metal ion is Cd (II), and Methylene Blue is the model organic pollutant. Although the variability and the variety of the experimental conditions in Tables 3 and 4 hinder a direct and accurate comparison between biosorbents, the corresponding results can be regarded as a platform for enhancing present knowledge on the continuous biosorption of pollutants for environmental remediation by further research.

The practical relevance of renewable resource biosorbents for large-scale applications in the continuous treatment of wastewater is also strongly conditioned by the degree to which they are able to preserve their efficiency during multiple cycles of repeated uses. Unfortunately, the biosorption-desorption studies aiming at biosorbent reusability assessment for removing heavy metals and organic pollutants are performed rarely and very rarely, respectively. The scarcity of data on the potential recyclability of the targeted biosorbents for heavy metal removal could be due to the limited number of column studies,

among which only around 35% address this issue. The data lack of pollutants of organic nature can also be explained on the basis of the complexity of the dynamic systems of biosorption involving organic species, in which some of the interactions between the surface functional groups of biosorbents and the organic molecules are not yet fully deciphered. As illustrative examples can be mentioned:

- Walnut shell functionalized with amino groups [199] and neem sawdust [200] that could be used for further fixed bed column removal of Cr(VI) even two and three cycles, respectively;
- *Chrysanthemum indicum* [201] with an efficiency of Co(II) desorption in continuous flow systems reduced by 12.3% after four cycles;
- Amino functionalized ramie stalk [202] with unchanged performances of fixed bed column biosorption of Cu(II) for five consecutive cycles;
- Chitosan (with 85% degree of deacetylation of chitin obtained from shrimp (*Penaeus brasiliensis*) waste) coated glass beads whose efficiency of Tartrazine and Sunset yellow dyes dynamic removal decreased from 36.3% in the first cycle to 33.8% after the fourth cycle [203]
- Agricultural waste biomass of *Nelumbo nucifera* immobilized in sodium silicate gel with the reusability of three cycles for Congo Red dye removal in dynamic systems [148].

For practical applications, the potential of the features of the continuous flow systems of biosorption pointed out in Tables 1–4 must be validated in competitive conditions by extensive research on simulated and real wastewaters. Although the very limited number of lab-scale studies available until now on this issue does not allow us to draw pertinent conclusions, their results are very encouraging. In the case of heavy metal ions removal by dynamic biosorption procedures, the most targeted are the real effluents from the electroplating industry. The works related to the biosorptive removal of organic pollutants in column mode are still in the infancy phase, the most interest being focused on the remediation of simulated wastewater contaminated with dyes [150]. The performances of the renewable resource biosorbents in the treatment of real wastewater by continuous biosorption processes are recorded in Table 5. The concentrations of the pollutants in the treated effluents in Table 5 have been reported as being quite far below the permissible limits.

**Table 5.** Renewable resource biosorbents for the removal of pollutants from real wastewater in continuous flow systems.

Biosorbent	Type of Real Wastewater	Targeted Pollutant; Influent Concentration of Pollutant	Working Conditions	Performances of the Fixed Bed Process	Ref.
Pristine lentile husk	Effluents from battery industry	Cd(II); 7.64 mg/L (effluent A); 7.78 mg/L (effluent B)	Fw = 20 mL/min; bed height = 10 cm; operation time: 6 h	Cd concentrations in the treated effluents: 0.48 mg/L (effluent A) and 0.58 mg/L (effluent B)	[203]
Neem sawdust	Tannery effluent	Cr(VI); 94 mg/L	Fw = 5 mL/min; bed height = 10 cm; pH = 2; 3 cycles	Percentage removal: 65.42% (1st cycle); 63.48% (2 rd cycle); 61.48% (3rd cycle)	[200]
3:2:1 combination of tea waste, maple leaves and mandarin peel	Semi-simulated real municipal wastewater	Cd(II); 20 mg/L Cu(II); 20 mg/L Pb(II); 20 mg/L Zn(II); 20 mg/L	Fw = 10 mL/min; bed height = 31 cm; pH = 2; particle size = 425–600 μm	Removal efficiency: >90% for all metals from 3227 (Cd), 2617(Cu), 1714 (Pb) and 2019 (Zn) mL of wastewater	[204]

Table 5. Cont.

Biosorbent	Type of Real Wastewater	Targeted Pollutant; Influent Concentration of Pollutant	Working Conditions	Performances of the Fixed Bed Process	Ref.
Lentil husk	Effluents from battery industry	Pb(II); 6.22 mg/L (effluent 1); 6.75 mg/L (effluent 2)	Fw = 20 mL/min; bed height = 10 cm; pH = 5; operation time: 6 h	Percentage of biosorption: 99.9% in the first 3 h (effluent 1) and 2 h (effluent 2), respectively; ~98% after 6 h	[205]
Acid treated <i>Lantana camara</i> fruits	Composite effluent from an electroplating industry	Cr(VI); 100 mg/L	Fw = 4 mL/min; bed height = 4 cm	Total effluent volume: 14.640 mL; removal efficiency: 59.2%; maximum bed capacity: 50.05 mg/g	[206]
Green coconut shells	Wastewater from electroplating industry	Ni(II); 2.787 mg/L; Zn(II); 98.02 mg/L; Cu(II); 320.4 mg/L	Fw = 20 mL/min; bed height = 10 cm; pH = 5	Saturation percentages: 83.42% (Ni); 71.45% (Zn); 56.40% (Cu); saturation volumes: 70 mL(Ni); 90 mL (Zn); 200 mL (Cu)	[207]
Acid-treated sugar cane bagasse	Wastewater from an electroplating factory	Cu(II); 200 mg/L; Ni(II); 14.4 mg/L; Zn(II); 65.5 mg/L	Fw = 2.0 mL/min; biosorbent mass: 4.0 g; pH = 1.26	Removal efficiency: -from wastewater with cyanide: 91.2%(Cu); 65.5%(Ni); 67%(Zn) -after cyanide removal 95.5%(Cu); 96.3%(Ni); 97.1%(Zn)	[208]
Chemically modified wood sawdust ( <i>Manilkara sp</i> ) (MS) and sugarcane bagasse (MB)	Electroplating wastewater	Zn(II); 70 mg/L	Fw = 15 mL/min; biosorbent mass: 3.0 g; pH = 6	Total Zn removal: 57.8 % (MS), 65.7% (MB); breakthrough volume: 2063 mL (MS), 1347 mL (MB);	[209]
Acid-treated crab shells	Electroplating industrial effluents	Ni(II); 109 mg/L (effluent 1) 52 mg/L (effluent 2)	Fw = 5 mL/min; bed height = 25 cm; pH = 7.48, 7.91	Efficiency of removal: 99.85% for a volume of effluent 1 of 4.38 L; 99.80% for 15.15 L of effluent 2	[210]
Jute/Polyacrylic acid hydrogel	Industrial effluent from a melting plant	Pb(II); 38.25 mg/L; Cd(II); 9.325 mg/L	2 consecutive fixed bed columns; Fw = 2.26 mL/min; bed height = 12 mm; pH = 2.8; 6 cycles	Concentrations of Pb and Cd in the treated effluent < 0.004 mg/L; volume of effluent: 32.8 L; breakthrough volumes: 3.96 L (Pb), 4.3 L (Cd)	[211]

Table 5. Cont.

Biosorbent	Type of Real Wastewater	Targeted Pollutant; Influent Concentration of Pollutant	Working Conditions	Performances of the Fixed Bed Process	Ref.
Shrimp shell waste	Coal acid mine drainage water	Fe ions (83.24 mg/L) Mn ions (14.70 mg/L)	continuous descendent flow; Fw = 7.8 mL/min; bed height = 34.5 cm; pH = 3.49; operating time: ≈180 min	Efficiency removal: Fe ions: up to 90% from which 52.5% has been identified as FeSO <sub>4</sub> Mn ions: 88% with 55.8% for Mn(II) Biosorption capacity: 17.43 mg/g (Fe), 3.87 mg/g (Mn) Percentage removal: 23.95%(Ni), 93.9%(Cu); column capacity: 12.841 mg/L (Ni), 6.1 mg/g (Cu) % Saturation: 50.1% (Cu), 50.1% (Ni); Zn (64.7%); breakthrough volume: 10 mL (Cu), 10 mL (Ni), 170 mL (Zn) <i>free NNLP</i> : R% = 76.25%; q = 8 mg/g; V <sub>eff</sub> = 0.18 L; t <sub>S</sub> = 3 h; t <sub>b</sub> = 0.375 h <i>immobilized NNLP</i> : R% = 62.18%; q = 5.84 mg/g; V <sub>eff</sub> = 0.135 L; t <sub>S</sub> = 2.25 h; t <sub>b</sub> = 0.2 h	[212]
Kola nut pod	Industrial paint effluent	Ni(II) (5.3747 mg/g) Cu(II) (35.6636 mg/g)	Fw = 5 mL/min; bed height = 10 cm		[213]
Cashew peduncle bagasse	Electroplating industry effluent	Cu(II) (61.16 mg/g) Ni(II) (3.97 mg/g) Zn(II) (47.70 mg/g)	Fw = 3 mL/min; bed height = 12 cm; pH = 5		[214]
free and sodium silicate gel-immobilized agricultural waste biomass of <i>Nelumbo nucifera</i> (lotus)-NNLP	industrial CR dye effluents	Congo red (CR)	In fixed-bed column was used free and sodium silicate gel-immobilized NNLP adsorbents. Fw = 1 mL/min; bed height = 2.5 cm; C <sub>0,dye</sub> = 215 mg/L;		[148]

## 6. Conclusions and Future Prospects

Renewable resource biosorbents possess good potential waiting to be valorized for the development of wastewater treatment technologies based on continuous biosorption processes. The restricted number of studies available until now that have been reviewed in the present work are carried out at a laboratory scale on fixed bed column systems and synthetic aqueous solutions of heavy metal ions and dyes. The addressed issues are related to the influence of the main operational parameters (initial concentration of pollutant, flow rate, and bed height), characterization of the dynamic systems of biosorption by means of breakthrough parameters, and modeling of breakthrough curves. Very little attention is paid to the aspects targeting the recyclability of biosorbents in continuous flow systems and their behavior in real industrial conditions. Therefore, extensive and in-depth research on this topic is imperatively necessary, especially in the following directions:

- Expanding and diversification of biosorbents, pollutants, and column biosorption procedures to be tested;
- The exploitation of the already obtained results on synthetic aqueous solutions to find the most suitable biosorbents for the treatment of real effluents in dynamic conditions;

- The transition from lab-scale studies to pilot- and full-scale studies;
- Assessment of the sustainability of the continuous flow systems of biosorption.

**Author Contributions:** Conceptualization, L.T. and D.S.; methodology, L.T. and D.S.; software, D.S.; validation, L.T.; formal analysis, L.T. and D.S.; investigation, L.T. and D.S.; resources, L.T. and D.S.; writing—original draft preparation, L.T. and D.S.; writing—review and editing, L.T. and D.S.; visualization, L.T. and D.S.; supervision, L.T. and D.S.; project administration, X.X L.T. and D.S.; All authors have read and agreed to the published version of the manuscript.

**Funding:** This research received no external funding.

**Data Availability Statement:** The data presented in this study are available on request from the corresponding author.

**Conflicts of Interest:** The authors declare no conflict of interest.

## References

1. Crini, G.; Lichtfouse, E. Advantages and disadvantages of techniques used for wastewater treatment. *Environ. Chem. Lett.* **2019**, *17*, 145–155. [[CrossRef](#)]
2. Saravanan, A.; Kumar, P.S.; Jeevanantham, S.; Karishma, S.; Tajsabreen, B.; Yaashikaa, P.R.; Reshma, B. Effective water/wastewater treatment methodologies for toxic pollutants removal: Processes and applications towards sustainable development. *Chemosphere* **2021**, *280*, 130595. [[CrossRef](#)] [[PubMed](#)]
3. Rodriguez-Narvaez, O.M.; Peralta-Hernandez, J.M.; Goonetilleke, A.; Bandala, E.R. Treatment technologies for emerging contaminants in water: A review. *Chem. Eng. J.* **2017**, *323*, 361–380. [[CrossRef](#)]
4. Somma, S.; Reverchon, E.; Baldino, L. Water purification of classical and emerging organic pollutants: An extensive review. *ChemEngineering* **2021**, *5*, 47. [[CrossRef](#)]
5. Saravanan, A.; Kumar, P.S.; Hemavathy, R.V.; Jeevanantham, S.; Harikumar, P.; Priyanka, G.; Devakirubai, D.R.A. A comprehensive review on sources, analysis and toxicity of environmental pollutants and its removal methods from water environment. *Sci. Total Environ.* **2021**, *812*, 152456. [[CrossRef](#)]
6. Akhtar, A.; Aslam, Z.; Asghar, A.; Bello, M.M.; Raman, A.A.A. Electrocoagulation of dye-containing wastewater: Optimization of operational parameters and process mechanism. *J. Environ. Chem. Eng.* **2020**, *8*, 104055. [[CrossRef](#)]
7. Dotto, G.L.; McKay, G. Current scenario and challenges in adsorption for water treatment. *J. Environ. Chem. Eng.* **2020**, *8*, 103988. [[CrossRef](#)]
8. Yousef, R.; Qiblawey, H.; El-Naas, M.H. Adsorption as a process for produced water treatment: A review. *Processes* **2020**, *8*, 1657. [[CrossRef](#)]
9. Rashid, R.; Shafiq, I.; Akhter, P.; Iqbal, M.J.; Hussain, M. A state-of-the-art review on wastewater treatment techniques: The effectiveness of adsorption method. *Environ. Sci. Pollut. Res.* **2021**, *28*, 9050–9066. [[CrossRef](#)]
10. Patel, H. Fixed-bed column adsorption study: A comprehensive review. *Appl. Water Sci.* **2019**, *9*, 45. [[CrossRef](#)]
11. Patel, H. Comparison of batch and fixed bed column adsorption: A critical review. *Int. J. Environ. Sci. Technol.* **2022**, *19*, 10409–10426. [[CrossRef](#)]
12. Ali, I. Water treatment by adsorption columns: Evaluation at ground level. *Sep. Purif. Rev.* **2014**, *43*, 175–205. [[CrossRef](#)]
13. Ahmed, M.J.; Hameed, B.H. Removal of emerging pharmaceutical contaminants by adsorption in a fixed-bed column: A review. *Ecotoxicol. Environ. Saf.* **2018**, *149*, 257–266. [[CrossRef](#)]
14. Malik, D.S.; Jain, C.K.; Yadav, A.K. Heavy Metal Removal by Fixed-Bed Column—A Review. *Chem. Bio. Eng. Rev.* **2018**, *5*, 173–179. [[CrossRef](#)]
15. Filote, C.; Roşca, M.; Hlihor, R.M.; Cozma, P.; Simion, I.M.; Apostol, M.; Gavrilescu, M. Sustainable application of biosorption and bioaccumulation of persistent pollutants in wastewater treatment: Current practice. *Processes* **2021**, *9*, 1696. [[CrossRef](#)]
16. Michalak, I.; Chojnacka, K.; Witek-Krowiak, A. State of the art for the biosorption process—A review. *Appl. Biochem. Biotechnol.* **2013**, *170*, 1389–1416. [[CrossRef](#)]
17. Ramírez Calderón, O.A.; Abdeldayem, O.M.; Pugazhendhi, A.; Rene, E.R. Current updates and perspectives of biosorption technology: An alternative for the removal of heavy metals from wastewater. *Curr. Pollut. Rep.* **2020**, *6*, 8–27. [[CrossRef](#)]
18. de Freitas, G.R.; da Silva, M.G.C.; Vieira, M.G.A. Biosorption technology for removal of toxic metals: A review of commercial biosorbents and patents. *Environ. Sci. Pollut. Res.* **2019**, *26*, 19097–19118. [[CrossRef](#)]
19. Vijayaraghavan, K.; Balasubramanian, R. Is biosorption suitable for decontamination of metal-bearing wastewaters? A critical review on the state-of-the-art of biosorption processes and future directions. *J. Environ. Manag.* **2015**, *160*, 283–296. [[CrossRef](#)]
20. Suteu, D.; Zaharia, C.; Malutan, T. Biosorbents based on lignin used in biosorption processes from wastewater treatment in Lignin. In *Properties and Applications in Biotechnology and Bioenergy*; Paterson, R.J., Ed.; Nova Science Publishers: New York, NY, USA, 2011; pp. 279–305.

21. Suteu, D.; Zaharia, C. Application of lignin materials for dye removal by sorption processes, In Lignin. In *Properties and Applications in Biotechnology and Bioenergy*; Paterson, R.J., Ed.; Nova Science Publishers: New York, NY, USA, 2011; pp. 477–488.
22. Suteu, D.; Zaharia, C.; Blaga, A.C. Biosorption-current bioprocess for wastewater treatment. In *Current Topics, Concepts and Research Priorities in Environmental Chemistry*; Zaharia, C., Ed.; Universitatii 'Al.I. Cuza' Publishing House: Iasi, Romania, 2012; Volume I, pp. 221–244.
23. da Costa, A.C.A.; Tavares, A.P.M.; de França, F.P. The release of light metals from a brown seaweed (*Sargassum* sp.) during zinc biosorption in a continuous system. *Electron. J. Biotechnol.* **2001**, *4*, 125–129. [[CrossRef](#)]
24. Antumes, W.M.; Luna, A.S.; Henriques, C.A.; daCosta, A.C.A. An Evaluation of Copper Biosorption by Brown Seaweed under Optimized Conditions. *Electron. J. Biotechnol.* **2003**, *6*, 174–184. [[CrossRef](#)]
25. Horsfall, M., Jr.; Spiff, A.I. Studies on the effect of pH on the sorption of Pb<sup>2+</sup> and Cd<sup>2+</sup> ions from aqueous solutions by *Caladium bicolor* (Wild Cocoyam) biomass. *Electron. J. Biotechnol.* **2004**, *7*, 313–323. [[CrossRef](#)]
26. Horsfall, M., Jr.; Spiff, A.I. Effects of temperature on the sorption of Pb<sup>2+</sup> and Cd<sup>2+</sup> from aqueous solution by *Caladium bicolor* (Wild Cocoyam) biomass. *Electron. J. Biotechnol.* **2005**, *8*, 162–169. [[CrossRef](#)]
27. Horsfall, M., Jr.; Spiff, A.I. Effect of metal ion concentration on the biosorption of Pb super(2+) and Cd super(2+) by *Caladium bicolor* (wild cocoyam). *Afr. J. Biotechnol.* **2005**, *4*, 191–196.
28. Ahalya, N.; Kanamadi, R.D.; Ramachandra, T.V. Biosorption of chromium (VI) from aqueous solutions by the husk of Bengal gram (*Cicer arietinum* sp.). *Electron. J. Biotechnol.* **2005**, *8*, 258–264. [[CrossRef](#)]
29. Nomanbhay, S.M.; Palanisamy, K. Removal of heavy metal from industrial wastewater using chitosan coated oil palm shell charcoal. *Electron. J. Biotechnol.* **2005**, *8*, 43–54. [[CrossRef](#)]
30. Bhatnagar, A.; Vilar, V.J.P.; Botelho, C.M.S.; Boaventura, R.A.R. Coconut-beased biosorbents for water treatment—A review of the recent literature. *Adv. Colloid Interface Sci.* **2010**, *160*, 1–15. [[CrossRef](#)]
31. Abdolati, A.; Guo, W.S.; Ngo, H.H.; Chen, S.S.; Nguyen, N.C.; Tnug, K.L. Typical lignocellulosic wastes and by-products for biosorption process in water and wastewater treatment: A critical review. *Bioresour. Technol.* **2014**, *160*, 57–66. [[CrossRef](#)]
32. Mo, J.; Yang, Q.; Zhang, N.; Zhang, W.; Zheng, Y.; Zhang, Z. A review on agro-industrial waste (AIW) derived adsorbents for water and wastewater treatment. *J. Environ. Manag.* **2018**, *227*, 395–405. [[CrossRef](#)]
33. Pavan-Kumar, G.U.S.R.; Malta, K.A.; Yerra, B.; Rao, K.S. Removal of Cu (II) using three low-cost adsorbents and prediction of adsorption using artificial neural networks. *Appl. Water Sci.* **2019**, *9*, 44–53. [[CrossRef](#)]
34. Okolo, B.I.; Oke, E.O.; Agu, C.M.; Nwosu-Obieogu, K.; Adeyi, O.; Akatobi, K.N. Development of new biosorbent materials from agricultural waste materials for the removal of Cd(II) ions from aqueous solution through the batch adsorption process. *Environ. Qual. Manag.* **2020**, *30*, 35–46. [[CrossRef](#)]
35. Elgarahy, A.M.; Elwakeel, K.Z.; Mohammad, S.H.; Elshoubaky, G.A. A critical review of biosorption of dyes, heavy metals and metalloids from wastewater as an efficient and green process. *Clean. Eng. Technol.* **2021**, *4*, 100209. [[CrossRef](#)]
36. Tanasa, A.; Suteu, D. Biovegetal wastes used as biosorbent for removal of chemical pollutants from wastewater. *Res. J. Agric. Sci.* **2021**, *53*, 227–232.
37. Gorduza, V.M.; Tofan, L.; Suteu, D.; Gorduza, E.V. *Biomateriale—Biotehnologii—Biocontrol*; Cermi Publishing House: Iasi, Romania, 2002.
38. Uddin, A.B.M.H.; Sujari, A.N.A.; Nawari, M.A.M. Effectiveness of peat coagulant for the removal of textile dyes from aqueous solution and textile wastewater. *Malays. J. Chem.* **2003**, *5*, 34–43.
39. Bhatnagar, A.; Jain, A.K. A comparative adsorption study with different industrial wastes as adsorbents for the removal of cationic dyes from water. *J. Colloid Interface Sci.* **2005**, *281*, 49–55. [[CrossRef](#)]
40. Allen, S.J.; Koumanova, B. Decolourisation of Water/Wastewater Using Adsorption. *J. Univ. Chem. Technol. Metall.* **2005**, *40*, 175–192.
41. Srivastava, V.C.; Swamy, M.M.; Mall, I.D.; Prasad, B.; Mishra, I.M. Adsorptive removal of phenol by bagasse fly ash and activated carbon: Equilibrium, kinetics and thermodynamics. *Colloids Surf. A Physicochem Eng. Aspects* **2006**, *272*, 89–104. [[CrossRef](#)]
42. Crini, G.; Badot, P.M. Application of chitosan, a natural aminopolysaccharide, for dye removal from aqueous solution by adsorption processes using batch studies: A review of recent literature. *Prog. Polym. Sci.* **2008**, *33*, 399–447. [[CrossRef](#)]
43. de Castro, K.C.; Cossolin, A.S.; Oliveira dos Reis, H.C.; Beraldo de Moraes, E. Biosorption of anionic textile dyes from aqueous solution by yeast slurry from brewery. *Braz. Archiv. Biol. Technol.* **2017**, *60*, e17160101. [[CrossRef](#)]
44. Mandal, A.; Singh, N.; Nain, L. Agro-waste biosorbents: Effect of physico-chemical properties on atrazine and imidacloprid sorption. *J. Environ. Sci. Health Part B* **2017**, *52*, 671–682. [[CrossRef](#)]
45. Zaharia, C.; Suteu, D. Textile organic dyes—Characteristics, polluting effects, and separation/elimination procedures from industrial effluents. A critical overview. In *Organic Pollutants—Ten Years after the Stockholm Convention—Environmental and Analytical Update*; Puzyn, T., Mostrag-Szlichtyng, A., Eds.; InTech Publisher: Rijeka, Croatia, 2012; pp. 55–86.
46. Contreras, E.; Sepulveda, L.; Palma, C. Valorization of Agroindustrial Wastes as Biosorbent for the Removal of Textile Dyes from Aqueous Solutions. *Int. J. Chem. Eng.* **2012**, *1*, 679352. [[CrossRef](#)]

47. Crominski da Silva, D.C.; Martins, J.; de Abreu Pietrobelli, T. Residual biomass of chia seeds (*Salvia hispanica*) oil extraction as low cost and eco-friendly biosorbent for effective reactive yellow B2R textile dye removal: Characterization, kinetic, thermodynamic and isotherm studies. *J. Environ. Chem. Eng.* **2019**, *7*, 103008. [[CrossRef](#)]
48. Stavrinou, A.; Aggelopoulos, C.A.; Tsakiroglou, C.D. Exploring the adsorption mechanisms of cationic and anionic dyes onto agricultural waste peels of banana, cucumber and potato: Adsorption kinetics and equilibrium isotherms as a tool. *J. Environ. Chem. Eng.* **2018**, *6*, 6958–6970. [[CrossRef](#)]
49. Khorasania, A.C.; Shojaosadatib, S.A. Magnetic pectin-*Chlorella vulgaris* biosorbent for the adsorption of dyes. *J. Environ. Chem. Eng.* **2019**, *7*, 103062. [[CrossRef](#)]
50. Adewuyi, A. Chemically modified biosorbents and their role in the removal of emerging pharmaceutical waste in the water system. *Water* **2020**, *12*, 1551. [[CrossRef](#)]
51. Bhattachar, C.; Dutta, S.; Saxena, V.K. A review on biosorptive removal of dyes and heavy metals from wastewater using watermelon rind as biosorbent. *Environ. Adv.* **2020**, *2*, 100007. [[CrossRef](#)]
52. Thirunavukkarasu, A.; Nithya, R.; Sivashankar, R. Continuous fixed-bed biosorption process: A review. *Chem. Eng. J. Adv.* **2021**, *8*, 100188. [[CrossRef](#)]
53. Kaplan, D.L. Introduction to Biopolymers from Renewable Resources. In *Biopolymers from Renewable Resources*; Kaplan, D.L., Ed.; Springer Publishing: Berlin, Germany, 1998.
54. Klemm, D.; Kramer, F.; Moritz, S.; Lindstrom, T.; Ankerfors, M.; Gray, D.; Dorris, A. Nanocelluloses: A new family of nature based materials. *Angew. Chem. Int. Ed.* **2011**, *50*, 5438–5463. [[CrossRef](#)]
55. Siro, D.; Plackett, D. Microfibrillated cellulose and new nanocomposite materials: A review. *Cellulose* **2010**, *17*, 459–494. [[CrossRef](#)]
56. Coseri, S. Insights on cellulose research in the last two decades in Romania. *Polymers* **2021**, *13*, 689. [[CrossRef](#)]
57. Lazzari, L.K.; Zampieri, V.B.; Neves, R.M.; Zanini, M.; Zattera, A.J.; Baldasso, C. A study on adsorption isotherm and kinetics of petroleum by cellulose cryogels. *Cellulose* **2019**, *26*, 1231–1246. [[CrossRef](#)]
58. Nica, I.; Zaharia, C.; Baron, R.I.; Coseri, S.; Suteu, D. Adsorptive materials based on cellulose: Preparation, characterization and applications for Cooper ions retention. *Cell. Chem. Technol.* **2020**, *54*, 579–590. [[CrossRef](#)]
59. Nica, I.; Biliuta, G.; Zaharia, C.; Rusu, L.; Coseri, S.; Suteu, D. Fixed-bed-column studies for methylene blue removal by cellulose cellets. *Environ. Eng. Manag. J.* **2020**, *19*, 269–279.
60. Iber, B.T.; Kasan, N.A.; Torsabo, D.; Omuwa, J.W. A review of various sources of chitin and chitosan in nature. *J. Renew. Mater.* **2022**, *10*, 1097–1123. [[CrossRef](#)]
61. Loth, F. *Industrial Gums: Polysaccharides and Their Derivatives*, 3rd ed.; Roy Whistler, L., Be Miller, J.N., Eds.; Academic Press Inc.: San Diego, CA, USA, 1993.
62. Bautista, J.; Jover, M.; Gutierrez, J.F.; Corpas, R.; Cremades, O.; Fontiveros, E.; Iglesias, F.; Vega, J. Preparation of crayfish chitin by in situ lactic acid production. *Process Biochem.* **2001**, *37*, 229–234. [[CrossRef](#)]
63. Ohno, N. *Yeast and Fungal Polysaccharides*, in *Comprehensive Glycoscience (From Chemistry to Systems Biology)*; Kamerling, H., Ed.; Elsevier Science: San Diego, CA, USA, 2007; Volume 2, Section II; pp. 559–577.
64. El-hefian, E.A.; Nasef, M.M.; Yahaya, A.H. Chitosan Physical Forms: A Short Review. *Aust. J. Basic Appl. Sci.* **2011**, *5*, 670–677.
65. Rizzi, Y.S.; Happel, P.; Lenz, S.; Urs, M.J.; Bonin, M.; Cord-Landwehr, S.; Singh, R.; Moerschbacher, B.M.; Kahmann, R. Chitosan and Chitin Deacetylase Activity Are Necessary for Development and Virulence of *Ustilago maydis*. *Mycology* **2021**, *12*, e03419-20. [[CrossRef](#)]
66. Duceac, I.A.; Tanasa, F.; Coseri, S. Selective Oxidation of Cellulose—A Multitask Platform with Significant Environmental Impact. *Materials* **2022**, *15*, 5076. [[CrossRef](#)]
67. Voudrias, E.; Fytianos, K.; Bozani, E. Sorption—Desorption isotherms of dyes from aqueous solutions and wastewaters with different sorbent materials. *Global Nest Int. J.* **2002**, *4*, 75–83.
68. Gavrilescu, M. Behaviour of persistent pollutants and risks associated with their presence in the environment—integrated studies. *Environ. Eng. Manag. J.* **2009**, *8*, 1517–1531. [[CrossRef](#)]
69. Bilal, M.; Rasheed, T.; Sosa-Hernandez, J.E.; Raza, A.; Nabeel, F.; Iqbal, H.M.N. Biosorption: An interplay between marine algae and potentially toxic elements—A review. *Mar. Drugs* **2018**, *16*, 65. [[CrossRef](#)]
70. Beni, A.; Esmaili, A. Biosorption, an efficient method for removing heavy metals from industrial effluents: A review. *Environ. Technol. Innov.* **2020**, *17*, 100503. [[CrossRef](#)]
71. Tanasa, A.; Puitel, A.C.; Zaharia, C.; Suteu, D. Sorption of reactive dyes from aqueous media using the lavender waste as biosorbent. *Desalin. Water Treat.* **2021**, *236*, 348–358. [[CrossRef](#)]
72. Hokkanen, S.; Bhatnagar, A.; Sillanpaa, M. A review on modification methods to cellulose-based adsorbents to improve adsorption capacity. *Water Res.* **2016**, *91*, 156–173. [[CrossRef](#)] [[PubMed](#)]
73. Deniz, F.; Karabulut, A. Biosorption of heavy metal ions by chemically modified biomass of coastal seaweed community: Studies on phytoremediation system modeling and design. *Ecol. Eng.* **2017**, *106*, 101–108. [[CrossRef](#)]
74. Lamaming, J.; Saalah, S.; Rajin, M.; Ismail, N.M.; Yaser, A.Z. A Review on Bamboo as an Adsorbent for Removal of Pollutants for Wastewater Treatment. *Int. J. Chem. Eng.* **2022**, *2022*, 7218759. [[CrossRef](#)]

75. Abegunde, S.M.; Idowu, K.S.; Adejuwon, O.M.; Adeyemi-Adejolu, T. A review on the influence of chemical modification on the performance of adsorbents, resources. *Environ. Sustain.* **2020**, *1*, 10001. [[CrossRef](#)]
76. Dostalek, P. Immobilized biosorbents for bioreactors and commercial biosorbents. In *Microbial Biosorption of Metals*; Kotrba, P., Mackova, M., Macek, T., Eds.; Springer: Berlin/Heidelberg, Germany, 2011.
77. Blaga, A.C.; Zaharia, C.; Suteu, D. Polysaccharides as Support for Microbial Biomass-Based Adsorbents with Applications in Removal of Heavy Metals and Dyes. Review. *Polymers* **2021**, *13*, 2893. [[CrossRef](#)]
78. Sarkheil, M.; Ameri, M.; Safari, O. Application of alginate-immobilized microalgae beads as biosorbent for removal of total ammonia and phosphorus from water of African cichlid (*Labidochromis lividus*) recirculating aquaculture system. *Environ. Sci. Pollut. Res.* **2022**, *29*, 11432–11444. [[CrossRef](#)]
79. Tran, V.S.; Ngo, H.H.; Hokkanen, W.; Zhang, J.; Liang, S.; Ton-That, C.; Zhang, X. Typical low cost biosorbents for adsorptive removal of specific organic pollutants from water. *Bioresour. Technol.* **2015**, *182*, 353–363. [[CrossRef](#)]
80. Kumar, R.; Sharma, R.K.; Singh, A.P. Cellulose based grafted biosorbents—Journey from lignocellulose biomass to toxic metal ions sorption applications—A review. *J. Mol. Liq.* **2017**, *232*, 62–93. [[CrossRef](#)]
81. Dhabhai, R.; Niu, C.H.; Dalai, A.K. Agricultural by products-based biosorbents for purification of bioalcohols: A review. *Bioresour. Bioprocess* **2018**, *5*, 37–51. [[CrossRef](#)]
82. Mahato, N.; Sharma, K.; Sinha, M.; Baral, E.R.; Koteswararao, R.; Dhyani, A.; Cho, M.H.; Cho, S. Bio-sorbents, industrially important chemicals and novel materials from citrus processing waste as a sustainable and renewable bioresource, A review. *J. Adv. Res.* **2020**, *23*, 61–82. [[CrossRef](#)] [[PubMed](#)]
83. Tanasa, F.; Teaca, C.A.; Nechifor, M. Lignocellulosic Waste Materials for Industrial Water Purification. In *Sustainable Green Chemical Processes and Their Allied Applications*; Inamuddin, A.A., Ed.; Springer: Cham, Switzerland, 2020; pp. 381–407.
84. Khadir, A.; Motamedi, M.; Pakzad, E.; Sillanpää, M.; Mahajan, S. The prospective utilization of Luffa fibres as a lignocellulosic bio-material for environmental remediation of aqueous media: A review. *J. Environ. Chem. Eng.* **2021**, *9*, 104691. [[CrossRef](#)]
85. Lee, H.V.; Hamid, S.B.A.; Zain, S.K. Conversion of lignocellulosic biomass to nanocellulose: Structure and chemical Process. *Sci. World J.* **2014**, *2014*, 63013. [[CrossRef](#)]
86. Isogai, A.; Bergström, L. Preparation of cellulose nanofibers using green and sustainable chemistry. *Curr. Opin. Green Sustain. Chem.* **2018**, *12*, 15–21. [[CrossRef](#)]
87. Ozel, N.; Elibol, M. A review on the potential uses of deep eutectic solvents in chitin and chitosan related processes. *Carbohydr. Polym.* **2021**, *262*, 117942. [[CrossRef](#)]
88. da Silva Lucas, A.J.; Oreste, E.Q.; Costa, H.L.G.; López, H.M.; Saad, C.D.M.; Prentice, C. Extraction, physicochemical characterization, and morphological properties of chitin and chitosan from cuticles of edible insects. *Food Chem.* **2021**, *343*, 128550. [[CrossRef](#)]
89. Wan Ngah, W.S.; Teong, L.C.; Hanafiah, M.A.K.M. Adsorption of dyes and heavy metal ions by chitosan composites: A review. *Carbohydr. Polym.* **2011**, *83*, 1446–1456. [[CrossRef](#)]
90. Crini, G.; Torri, G.; Lichtfouse, E.; Kyzas, G.Z.; Wilson, L.D.; Morin-Crini, N. Dye removal by biosorption using cross-linked chitosan-based hydrogels. *Environ. Chem. Lett.* **2019**, *17*, 1645–1666. [[CrossRef](#)]
91. Peter, S.; Lyczko, N.; Gopakumar, D.; Maria, H.J.; Nzihou, A.; Thomas, S. Chitin and Chitosan Based Composites for Energy and Environmental Applications: A Review. *Waste Biomass Valorization* **2021**, *12*, 4777–4804. [[CrossRef](#)]
92. Rodriguez-Rodriguez, R.; Espinosa-Andrews, H.; Velasquillo-Martinez, C.; Garcia-Carvajal, Z.Y. Composite hydrogel based on gelatin, chitosan and polyvinyl alcohol to biomedical application: A review. *Int. J. Polym. Mater. Polym. Biomater.* **2020**, *69*, 1–20. [[CrossRef](#)]
93. Tahira, I.; Aslam, Z.; Abbas, A.; Monim-ul-Mehboob, M.; Ali, S.; Asghar, A. Adsorptive removal of acidic dye onto grafted chitosan: A plausible grafting and adsorption mechanism. *Int. J. Biol. Macromol.* **2019**, *136*, 1209–1218. [[CrossRef](#)]
94. Wang, B.; Sun, Y.-C.; Sun, R.-C. Fractionation and structural characterization of lignin and its modification as biosorbents for efficient removal of chromium from wastewater: A review. *J. Leather Sci. Eng.* **2019**, *1*, 5. [[CrossRef](#)]
95. Ahmed, M.J.; Hameed, B.H.; Hummadi, E.H. Review on recent progress in chitosan/chitin-carbonaceous material composites for the adsorption of water pollutants. *Carbohydr. Polym.* **2020**, *247*, 116690. [[CrossRef](#)]
96. Ayub, A.; Srithilat, K.; Fatima, I.; Panduro-Tenazoa, N.M.; Ahmed, I.; Akhtar, M.U.; Shabbir, W.; Ahmad, K.; Muhammad, A. Arsenic in drinking water: Overview of removal strategies and role of chitosan biosorbent for its remediation. *Environ. Sci. Pollut. Res.* **2022**, *29*, 64312–64344. [[CrossRef](#)]
97. Sarode, S.; Upadhyay, P.; Khosa, M.A.; Mak, T.; Shakir, A.; Song, S.; Ullah, A. Overview of wastewater treatment methods with special focus on biopolymer chitin-chitosan. *Int. J. Biol. Macromol.* **2019**, *121*, 1086–1100. [[CrossRef](#)]
98. Maliki, S.; Sharma, G.; Kumar, A.; Moral-Zamorano, M.; Moradi, O.; Baselga, J.; Stadler, F.J.; García-Peñas, A. Chitosan as a Tool for Sustainable Development: A Mini Review. *Polymers* **2022**, *14*, 1475. [[CrossRef](#)]
99. Kurecic, M.; Smole, M.S. Polymer Nanocomposite Hydrogel for Water Purification. In *Nanocomposites—New Trends and Development*; Ebrahimi, F., Ed.; InechOpen: Rijeka, Croatia, 2012.
100. Ullah, F.; Othman, M.B.H.; Javed, F.; Ahmad, Z.; Akil, H.M. Classification, processing and application of hydrogels: A review. *Mater. Sci. Eng. C* **2015**, *57*, 414–433. [[CrossRef](#)]

101. Varaprasad, K.; Raghavendra, G.M.; Jayaramudu, T.; Yallapu, M.M.; Sadiku, R. A mini review on hydrogels classification and recent developments in miscellaneous application. *Mater. Sci. Eng.* **2017**, *79*, 958–971. [[CrossRef](#)]
102. Shalla, A.H.; Yaseen, Z.; Bhat, M.A.; Rangreez, A.; Maswall, M. Recent review for removal of metal ions by hydrogel. *Sep. Sci. Technol.* **2019**, *54*, 89–100. [[CrossRef](#)]
103. Bashir, S.; Hina, M.; Igbal, J.; Rajpar, A.H.; Mujtaba, M.A.; Alghamdi, N.A.; Wageh, S.; Ramesh, K.; Ramesh, S. Fundamental Concepts of Hydrogels: Synthesis, Properties and their Applications. *Polymers* **2009**, *12*, 2702. [[CrossRef](#)] [[PubMed](#)]
104. Akter, M.; Bhattacharjee, M.; Dhar, A.K.; Rahman, F.B.A.; Haque, S.; Rashid, T.U.; Kabir, S.M.F. Cellulose-Based Hydrogels for Wastewater Treatment: A Concise Review. *Gels* **2021**, *7*, 30. [[CrossRef](#)] [[PubMed](#)]
105. Haque, M.O.; Mondal, M.I.H. Synthesis and Characterization of Cellulose-based Eco-Friendly Hydrogels. *Rajshahi Univ. J. Sci. Eng.* **2016**, *44*, 45–53. [[CrossRef](#)]
106. Akalin, G.O.; Pulat, M. Preparation of sodium carboxymethyl cellulose-based hydrogel for controlled release of copper micronutrient. *Euroasia Proc. Sci. Eng. Math.* **2018**, *2*, 25.
107. Jayaramudu, T.; Ko, H.U.; Kim, H.C.; Kim, J.W.; Kim, J. Swelling behavior of polyacrylamide-cellulose nanocrystal hydrogel: Swelling kinetics, temperature, and pH effects. *Materials* **2019**, *12*, 2080. [[CrossRef](#)]
108. Ahmed, E.M. Hydrogel: Preparation, characterization and application: A review. *J. Adv. Res.* **2015**, *6*, 105–121. [[CrossRef](#)]
109. Ma, S.; Yu, B.; Pei, X.; Zhou, F. Structural hydrogels. *Polymer* **2016**, *98*, 516–535. [[CrossRef](#)]
110. Aktar, M.F.; Hanif, M.; Ranjha, N.M. Methods of synthesis of hydrogel. A review. *Sandi Pharm. J.* **2016**, *24*, 554–559. [[CrossRef](#)]
111. Kundu, R.; Mahada, P.; Chhiang, B.; Das, B. Cellulose hydrogel: Green and sustainable soft biomaterials. *Curr. Res. Green Sustain. Chem.* **2022**, *5*, 100252. [[CrossRef](#)]
112. Tien, C. *Introduction to Adsorption: Basics, Analysis and Applications*; Elsevier: Amsterdam, The Netherlands, 2018.
113. Volensky, B. *Biosorption of Heavy Metals*; CRC Press: Boca Raton, FL, USA, 1990.
114. Worch, E. Adsorption technology in water treatment. In *Adsorption Technology in Water Treatment*; Walter de Gruyter GmbH & Co. KG: Berlin, Germany, 2021.
115. Kamar, F.H.; Mohammed, A.A.; Faisal, A.A.; Nechifor, A.C.; Nechifor, G. Biosorption of lead, copper and cadmium ions from industrial wastewater using fluidized bed of dry cabbage leaves. *Rev. Chim.* **2016**, *67*, 1039–1046.
116. Al-Baidhani, J.H.; Al-Salihy, S.T. Removal of heavy metals from aqueous solution by using low cost rice husk in batch and continuous fluidized experiments. *Int. J. Chem. Eng. Appl.* **2016**, *7*, 6–10. [[CrossRef](#)]
117. Hummadi, K.K.; Luo, S.; He, S. Adsorption of methylene blue dye from the aqueous solution via bio-adsorption in the inverse fluidized-bed adsorption column using the torrefied rice husk. *Chemosphere* **2022**, *287*, 131907. [[CrossRef](#)]
118. Tofan, L.; Bojoaga, C.N.; Paduraru, C. Biosorption the recovery and analysis of rare earth elements and platinum group metals from real samples. A review. *Environ. Chem. Lett.* **2022**, *20*, 1225–1248. [[CrossRef](#)]
119. Aksu, Z. Application of biosorption for the removal of organic pollutants: A review. *Process Biochem.* **2005**, *40*, 997–1026. [[CrossRef](#)]
120. Das, N.; Das, D. Recovery of rare earth metals through biosorption: An overview. *J. Rare Earth* **2013**, *31*, 933–943. [[CrossRef](#)]
121. Park, D.; Yun, Y.-S.; Park, J.M. The past, present and future trends of biosorption. *Biotechnol. Bioprocess Eng.* **2010**, *15*, 86–102. [[CrossRef](#)]
122. Rosales, E.; Meijide, J.; Pazos, M.; Sanroman, A. Challenges and recent advances in biochar as low-cost biosorbent: From batch assays to continuous flow systems. *Bioresour. Technol.* **2017**, *246*, 176–192. [[CrossRef](#)]
123. da Costa, T.B.; da Silva, M.G.C.; Vieira, M.G.A. Recovery of rare earth metals from aqueous solutions by bio/adsorption using non-conventional materials: A review with recent studies and promising approaches in column applications. *J. Rare Earths* **2020**, *38*, 339–355. [[CrossRef](#)]
124. Kafshgari, F.; Keshtkar, A.R.; Mousavian, M.A. Study of Mo (VI) removal from aqueous solution: Application of different mathematical models to continuous biosorption data. *Iran. J. Env. Health Sci. Eng.* **2013**, *10*, 14. [[CrossRef](#)]
125. Miralles, N.; Valderrama, C.; Casas, I.; Martínez, M.; Florido, A. Cadmium and Lead Removal from Aqueous Solution by Grape Stalk Wastes: Modeling of a Fixed-Bed Column. *J. Chem. Eng. Data* **2010**, *55*, 3548–3554. [[CrossRef](#)]
126. Tofan, L.; Paduraru, C.; Teodosiu, C.; Toma, O. Fixed bed column study on the removal of chromium (III) ions from aqueous solutions by using hemp fibers with improved sorption performance. *Cellul. Chem. Technol.* **2015**, *49*, 219–229.
127. Mazouz, R.; Filali, N.; Hattab, Z.; Guerfi, K. Valorization of granulated slag of Arcelor-Mittal (Algeria) in cationic dye adsorption from aqueous solution: Column studies. *J. Water Reuse Desalin.* **2016**, *6*, 204–213. [[CrossRef](#)]
128. Cruz-Olivares, J.; Pérez-Alonso, C.; Barrera-Díaz, C.; Ureña-Núñez, F.; Chaparro-Mercado, M.C.; Bilyeu, B. Modeling of lead (II) biosorption by residue of allspice in a fixed-bed column. *Chem. Eng. J.* **2013**, *228*, 21–27. [[CrossRef](#)]
129. Kulkarni, R.M.; Dhanyshree, J.K.; Varma, E.; Sirivibha, S.P. Batch and continuous packed bed column studies on biosorption of nickel(II) by sugarcane bagasse. *Results Chem.* **2022**, *4*, 100328. [[CrossRef](#)]
130. Davila-Guzman, N.E.; Cerino-Córdova, F.D.J.; Loredó-Cancino, M.; Rangel-Mendez, J.R.; Gómez-González, R.; Soto-Regalado, E. Studies of adsorption of heavy metals onto spent coffee ground: Equilibrium, regeneration, and dynamic performance in a fixed-bed column. *Int. J. Chem. Eng.* **2016**, *2016*, 9413879. [[CrossRef](#)]
131. Chen, S.; Yue, Q.; Gao, B.; Li, Q.; Xu, X.; Fu, K. Adsorption of hexavalent chromium from aqueous solution by modified corn stalk: A fixed-bed column study. *Bioresour. Technol.* **2012**, *113*, 114–120. [[CrossRef](#)]

132. Yahya, M.D.; Aliyu, A.S.; Obayomi, K.S.; Olugbenga, A.G.; Abdullahi, U.B. Column adsorption study for the removal of chromium and manganese ions from electroplating wastewater using cashew nutshell adsorbent. *Cogent Eng.* **2020**, *7*, 1748470. [[CrossRef](#)]
133. Maheshwari, U.; Gupta, S. Removal of Cr (VI) from wastewater using activated neem bark in a fixed-bed column: Interference of other ions and kinetic modelling studies. *Desalin. Water Treat.* **2016**, *57*, 8514–8525. [[CrossRef](#)]
134. Chatterjee, A.; Schiewer, S. Effect of competing cations (Pb, Cd, Zn, and Ca) in fixed-bed column biosorption and desorption from citrus peels. *Water Air Soil Pollut.* **2014**, *225*, 1854. [[CrossRef](#)]
135. Rodrigues, J.A.V.; Martins, L.R.; Furtado, L.M.; Xavier, A.L.P.; Almeida, F.T.R.D.; Moreira, A.L.D.S.L.; Sacramento Melo, T.A.; Gil, F.L.; Gurgel, L.V.A. Oxidized renewable materials for the removal of cobalt (II) and copper (II) from aqueous solution using in batch and fixed-bed column adsorption. *Adv. Polym. Technol.* **2020**, *2020*, 8620431. [[CrossRef](#)]
136. Hanafiah, M.A.K.M.; Zakaria, H.; Ngah, W.S.W. Base Treated Cogon Grass (*Imperata cylindrica*) as an Adsorbent for the Removal of Ni (II): Kinetic, Isothermal and Fixed-bed Column Studies. *Clean-Soil Air Water* **2010**, *38*, 248–256. [[CrossRef](#)]
137. Danish, M.; Ansari, K.B.; Danish, M.; Khan, N.A.; Aftab, R.A.; Zaidi, S.; Khan, M.S.; Al Mesfer, M.K.; Qyyum, M.A.; Nizami, A.S. Developing convective–dispersive transport model to characterize fixed-bed adsorption of lead (II) over activated tea waste biosorbent. *Biomass Conv. Bioref.* **2022**, *12*, 4291–4305. [[CrossRef](#)]
138. Harripersadth, C.; Musonge, P. The Dynamic Behaviour of a Binary Adsorbent in a Fixed Bed Column for the Removal of Pb<sup>2+</sup> Ions from Contaminated Water Bodies. *Sustainability* **2022**, *14*, 7662. [[CrossRef](#)]
139. Masukume, M.; Onyango, M.S.; Maree, J.P. Sea shell derived adsorbent and its potential for treating acid mine drainage. *Int. J. Miner. Process.* **2014**, *133*, 52–59. [[CrossRef](#)]
140. Aranda-García, E.; Cristiani-Urbina, E. Effect of pH on hexavalent and total chromium removal from aqueous solutions by avocado shell using batch and continuous systems. *Environ. Sci. Pollut. Res.* **2019**, *26*, 3157–3173. [[CrossRef](#)]
141. Li, C.; Champagne, P. Fixed-bed column study for the removal of cadmium (II) and nickel (II) ions from aqueous solutions using peat and mollusk shells. *J. Hazard. Mater.* **2009**, *171*, 872–878. [[CrossRef](#)]
142. Du, Z.; Zheng, T.; Wang, P. Experimental and modelling studies on fixed bed adsorption for Cu (II) removal from aqueous solution by carboxyl modified jute fiber. *Powder Technol.* **2018**, *338*, 952–959. [[CrossRef](#)]
143. Wang, F.; Yu, J.; Zhang, Z.; Xu, Y.; Chi, R. An amino-functionalized ramie stalk-based adsorbent for highly effective Cu<sup>2+</sup> removal from water: Adsorption performance and mechanism. *Process Saf. Environ. Prot.* **2018**, *117*, 511–522. [[CrossRef](#)]
144. Lakshmiopathy, R.; Sarada, N.C. A fixed bed column study for the removal of Pb<sup>2+</sup> ions by watermelon rind. *Environ. Sci. Water Res. Technol.* **2015**, *1*, 244–250. [[CrossRef](#)]
145. Borna, M.O.; Pirsahab, M.; Niri, M.V.; Mashizie, R.K.; Kakavandi, B.; Zare, M.R.; Asadi, A. Batch and column studies for the adsorption of chromium (VI) on low-cost Hibiscus Cannabinus kenaf, a green adsorbent. *J. Taiwan Inst. Chem. Eng.* **2016**, *68*, 80–89. [[CrossRef](#)]
146. Abrouki, Y.; Mabroukia, J.; Anouzla, A.; Rifi, S.K.; Zahiria, Y.; Nehhala, S.; El Yadinia, A.; Slimania, R.; El Hajjajia, S.; Loukilib, H.; et al. Optimization and modeling of a fixed-bed biosorption of textile dye using agricultural biomass from the Moroccan Sahara. *Des. Water Treat.* **2021**, *240*, 144–151. [[CrossRef](#)]
147. Mohammed, N.; Grishkewich, N.; Waeijen, H.A.; Berry, R.M.; Tam, K.C. Continuous flow adsorption of methylene blue by cellulose nanocrystal-alginate hydrogel beads in fixed bed columns. *Carbohydr. Polym.* **2016**, *136*, 1194–1202. [[CrossRef](#)] [[PubMed](#)]
148. Parimelazhagan, V.; Jeppu, G.; Rampal, N. Continuous Fixed-Bed Column Studies on Congo Red Dye Adsorption-Desorption Using Free and Immobilized *Nelumbo nucifera* Leaf Adsorbent. *Polymers* **2022**, *14*, 54. [[CrossRef](#)] [[PubMed](#)]
149. Józwiak, T.; Filipkowska, U. The use of air-lift adsorber with a floating filling from a cross-linked chitosan hydrogels for Reactive Black 5 removal. *Sci. Rep.* **2021**, *11*, 13382. [[CrossRef](#)]
150. Verduzco-Navarro, I.P.; Jasso-Gastinel, C.F.; Rios-Donato, N.; Mendizábal, E. Red dye 40 removal by fixed-bed columns packed with alginate-chitosan sulfate hydrogels Remoción del colorante rojo 40 por medio de columnas de lecho fijo empacadas con hidrogeles de alginato-sulfato de quitosano. *Rev. Mex. Ing. Química* **2020**, *19*, 1401–1411. [[CrossRef](#)]
151. Chu, K.H. Breakthrough curve analysis by simplistic models of fixed bed adsorption: In defense of the century-old Bohart-Adams model. *Chem. Eng. J.* **2020**, *380*, 122513. [[CrossRef](#)]
152. Chu, K.H. Fixed bed sorption: Setting the record straight on the Bohart–Adams and Thomas models. *J. Hazard. Mater.* **2010**, *177*, 1006–1012. [[CrossRef](#)]
153. Thomas, H.C. Heterogeneous ion exchange in a flowing system. *J. Am. Chem. Soc.* **1944**, *66*, 1466–1664. [[CrossRef](#)]
154. Yoon, Y.H.; Nelson, J.H. Application of Gas Adsorption Kinetics I. A Theoretical Model for Respirator Cartridge Service Life. *Am. Ind. Hyg. Assoc. J.* **1984**, *45*, 509–516. [[CrossRef](#)]
155. Bohart, G.S.; Adams, E.Q. Some aspects of the behavior of charcoal with respect to chlorine. *J. Am. Chem. Soc.* **1920**, *42*, 523–544. [[CrossRef](#)]
156. Mckay, G.; Bino, M.J. Fixed bed adsorption for the removal of pollutants from water. *Environ. Pollut.* **1990**, *66*, 33–53. [[CrossRef](#)]
157. Clark, R.M. Evaluating the cost and performance of field-scale granular activated carbon systems. *Environ. Sci. Technol.* **1987**, *21*, 573–580. [[CrossRef](#)]
158. Wolborska, A. Adsorption on activated carbon of *p*-nitrophenol from aqueous solution. *Water Res.* **1989**, *23*, 85–91. [[CrossRef](#)]
159. Yan, G.; Viraraghavan, T.; Chen, M. A new model for heavy metal removal in a biosorption column. *Adsorp. Sci. Technol.* **2001**, *19*, 25–43. [[CrossRef](#)]

160. Xavier, A.L.P.; Adarme, O.F.H.; Furtado, L.M.; Ferreira, G.M.D.; Mendes da Silva, L.H.; Gil, L.F.; Gurgel, L.V.A. Modeling adsorption of copper(II), cobalt(II) and nickel(II) metal ions from aqueous solution onto a new carboxylated sugarcane bagasse. Part II: Optimization of monocomponent fixed-bed column adsorption. *J. Colloid Interface Sci.* **2018**, *516*, 431–445. [[CrossRef](#)]
161. Xu, Z.; Cai, J.-G.; Pan, B.-C. Mathematically modeling fixed-bed adsorption in aqueous systems. *J. Zhejiang Univ. Sci. A* **2013**, *14*, 155–176. [[CrossRef](#)]
162. Duga, N.D.F.; Imperial, P.E.A.; Soriano, A.N.; Nieva, A.D. Packed bed biosorption of lead and copper ions using sugarcane bagasse. *ASEAN J. Chem. Eng.* **2016**, *16*, 23–37. [[CrossRef](#)]
163. Vera, L.M.; Bermejo, D.; Uguña, M.F.; Garcia, N.; Flores, M.; González, E. Fixed bed column modeling of lead(II) and cadmium(II) ions biosorption on sugarcane bagasse. *Environ. Eng. Res.* **2019**, *24*, 31–37. [[CrossRef](#)]
164. Chao, H.P.; Chang, C.C.; Nieva, A. Biosorption of heavy metals on Citrus maxima peel, passion fruit shell, and sugarcane bagasse in a fixed-bed column. *J. Ind. Eng. Chem.* **2014**, *20*, 3408–3414. [[CrossRef](#)]
165. Soetaredjo, F.E.; Kurniawan, A.; Ong, L.K.; Widagdyo, D.R.; Ismajji, S. Investigation of the continuous flow sorption of heavy metals in a biomass-packed column: Revisiting the Thomas design model for correlation of binary component systems. *RSC Adv.* **2014**, *4*, 52856–52870. [[CrossRef](#)]
166. Muhamad, H.; Doan, H.; Lohi, A. Batch and continuous fixed bed column biosorption of Cu<sup>2+</sup> and Cd<sup>2+</sup>. *Chem. Eng. J.* **2010**, *158*, 369–377. [[CrossRef](#)]
167. Sharma, R.; Singh, B. Removal of Ni (II) ions from aqueous solutions using modified rice straw in a fixed bed column. *Bioresour. Technol.* **2013**, *146*, 519–524. [[CrossRef](#)] [[PubMed](#)]
168. Cheraghi, E.; Ameri, E.; Moheb, A. Continuous biosorption of Cd (II) ions from aqueous solutions by sesame waste: Thermodynamics and fixed-bed column studies. *Desalin. Water Treat.* **2016**, *57*, 6936–6949. [[CrossRef](#)]
169. Banerjee, M.; Bar, N.; Basu, R.K.; Das, S.K. Removal of Cr(VI) from its aqueous solution using green adsorbent, pistachio shell: A fixed bed column study and GA-ANN modeling. *Water Conser. Sci. Eng.* **2018**, *3*, 19–31. [[CrossRef](#)]
170. Aranda-García, E.; Cristiani-Urbina, E. Hexavalent chromium removal and total chromium biosorption from aqueous solution by *Quercus crassipes* acorn shell in a continuous up-flow fixed-bed column: Influencing parameters, kinetics, and mechanism. *PLoS ONE* **2020**, *15*, e0227953. [[CrossRef](#)]
171. Mitra, T.; Bar, N.; Das, S.K. Rice husk: Green adsorbent for Pb (II) and Cr (VI) removal from aqueous solution—Column study and GA-NN modeling. *SN Appl. Sci.* **2019**, *1*, 486. [[CrossRef](#)]
172. Garba, A.; Nasu, N.M.; Basri, H.; Zain, H.M.; Hayatu, U.S.; Abdulrasheed, A.; Mohsin, R.; Majid, Z.A.; Rashid, N.M. Modelling of Cd(II) uptake from aqueous solutions using treated rice husk: Fixed bed column studies. *Chem. Eng. Trans.* **2017**, *56*, 229–234. [[CrossRef](#)]
173. Chatterjee, A.; Schiewer, S. Biosorption of cadmium (II) ions by citrus peels in a packed bed column: Effect of process parameters and comparison of different breakthrough curve models. *Clean-Soil Air Water* **2011**, *39*, 874–881. [[CrossRef](#)]
174. Acheampong, M.A.; Pakshirajan, K.; Annachhatre, A.P.; Lens, P.N. Removal of Cu (II) by biosorption onto coconut shell in fixed-bed column systems. *J. Ind. Eng. Chem.* **2013**, *19*, 841–848. [[CrossRef](#)]
175. Kumar, S.; Patra, C.; Narayanasamy, S.; Rajamaran, P.V. Performance of acid-activated water caltrop (*Trapa natans*) shell in fixed bed column for hexavalent chromium removal from simulated wastewater. *Environ. Sci. Pollut. Res.* **2020**, *27*, 28042–28052. [[CrossRef](#)]
176. Teixeira, R.N.; Neto, V.O.S.; Oliveira, J.T.; Oliveira, T.C.; Melo, D.Q.; Silva, M.A.; Nascimento, R.F. Study on the use of roasted barley powder for adsorption of Cu<sup>2+</sup> ions in batch experiments and in fixed-bed columns. *Bioresources* **2013**, *8*, 3556–3573. [[CrossRef](#)]
177. Agrawal, P.; Rao, N.N.; Sharma, A.; Hiremath, L.; Tippareddy, K.S. Modelling and efficiency assessment of the up flow fixed bed process packed with Moringa oleifera for continuous Cd (II) removal from drinking water. *J. Mol. Struct.* **2021**, *1236*, 130328. [[CrossRef](#)]
178. Hymavathi, D.; Prabhakar, G. Modeling of cobalt and lead adsorption by *Ficus benghalensis* L. in a fixed bed column. *Chem. Eng. Commun.* **2019**, *206*, 1264–1272. [[CrossRef](#)]
179. Mitra, T.; Das, S.K. Cr (VI) removal from aqueous solution using *Psidium guajava* leaves as green adsorbent: Column studies. *Appl. Water Sci.* **2019**, *9*, 153. [[CrossRef](#)]
180. Hasfalina, C.M.; Maryam, R.Z.; Luqman, C.A.; Rashid, M. Adsorption of copper (II) from aqueous medium in fixed-bed column by kenaf fibres. *APCBEE Procedia* **2012**, *3*, 255–263. [[CrossRef](#)]
181. Al-Shawabkeh, A.F.; Omarb, W.; Haseinec, A.; Al-Amayreh, M. Experimental study of the application of date palm trunk fiber as biosorbent for removal cadmium using a fixed bed column: Investigation of the influence of particle size. *Desalin. Water Treat.* **2021**, *223*, 328–334. [[CrossRef](#)]
182. Vijayaraghavan, K.; Thilakavathi, M.; Palanivelu, K.; Velan, M. Continuous sorption of copper and cobalt by crab shell particles in a packed column. *Environ. Technol.* **2005**, *26*, 267–276. [[CrossRef](#)]
183. Nguyen, T.A.; Nhana, C.H.; Lea, M.V.; Huynh, P.H.K.; Phungb, T.K.; Tranc, A.V. Fixed Bed Column Studies for the Adsorption of Cadmium onto Cockle Shell (*Anadara Granosa*) Powder. *Chem. Eng. Trans.* **2021**, *83*, 259–264. [[CrossRef](#)]
184. Van, H.T.; Nguyen, L.H.; Nguyen, X.H.; Nguyen, T.H.; Nguyen, T.V.; Vigneswaran, S.; Rinklebe, J.; Tran, H.N. Characteristics and mechanisms of cadmium adsorption onto biogenic aragonite shells-derived biosorbent: Batch and column studies. *J. Environ. Manag.* **2019**, *241*, 535–548. [[CrossRef](#)]

185. Al-Zawahreh, K.; Barral, M.T.; Al-Degs, Y.; Paradelo, R. Competitive removal of textile dyes from solution by pine bark-compost in batch and fixed bed column experiments. *Environ. Technol. Innov.* **2022**, *27*, 102421. [[CrossRef](#)]
186. Bharathi, K.S.; Ramesh, S.P.T. Fixed-bed column studies on biosorption of crystal violet from aqueous solution by *Citrullus lanatus* rind and *Cyperus rotundus*. *Appl. Water Sci.* **2013**, *3*, 673–687. [[CrossRef](#)]
187. Charola, S.; Yadav, R.; Das, P.; Maiti, S. Fixed-bed adsorption of Reactive Orange 84 dye onto activated carbon prepared from empty cotton flower agro-waste. *Sustain. Environ. Res.* **2018**, *28*, 298–308. [[CrossRef](#)]
188. Djelloula, C.; Hamdaoui, O. Dynamic adsorption of methylene blue by melon peel in fixed-bed columns. *Desalin. Water Treat.* **2014**, *56*, 2966–2975. [[CrossRef](#)]
189. Patel, H.; Vashi, R.T. Fixed bed column adsorption of ACID Yellow 17 dye onto Tamarind Seed Powder. *Can. J. Chem. Eng.* **2012**, *90*, 180–185. [[CrossRef](#)]
190. Gupta, V.K.; Tyagi, I.; Agarwal, S.; Singh, R.; Chaudhary, M.; Harit, A.; Kushwaha, S. Column operation studies for the removal of dyes and phenols using a low cost adsorbent. *Global J. Environ. Sci. Manag.* **2016**, *2*, 1–10. [[CrossRef](#)]
191. González-López, M.E.; Laureano-Anzaldo, C.M.; Pérez-Fonseca, A.A.; Gómez, C.; Robledo-Ortiz, J.R. Congo red adsorption with cellulose-graphene nanoplatelets beads by differential column batch reactor. *J. Environ. Chem. Eng.* **2021**, *9*, 105029. [[CrossRef](#)]
192. Bencheqroun, Z.; Nawdali, M.; El Mrabet, I.; Tanji, K.; Majdoub, M.; Zaitan, H. Fixed-Bed System for Adsorption of Methylene Blue and Congo Red Dyes onto *Cupressus sempervirens*: Single- and Multi-Solute Systems. *Lett. Appl. NanoBioSci.* **2023**, *12*, 106. [[CrossRef](#)]
193. López-Cervantes, J.; Sánchez-Machado, D.I.; Sánchez-Duarte, R.G.; Murrieta, M.A.C. Study of a fixed-bed column in the adsorption of an azo dye from an aqueous medium using a chitosan–glutaraldehyde biosorbent. *Adsorpt. Sci. Technol.* **2018**, *36*, 215–232. [[CrossRef](#)]
194. Rouf, S.; Nagapadma, M. Impregnated with a Cationic Surfactant Modeling of Fixed Bed Column Studies for Adsorption of Azo Dye on Chitosan. *Int. J. Sci. Eng. Res.* **2015**, *6*, 538–545. [[CrossRef](#)]
195. Francis, A.O.; Zaini, M.A.A.; Muhammad, I.M.; Abdulsalam, S.; El-Nafaty, U.A. Adsorption dynamics of dye onto crab shell chitosan/neem leaf Composite. *Water Pract. Technol.* **2020**, *15*, 673–682. [[CrossRef](#)]
196. Nguyen, T.A.; Nguyen, V.T.; Tran, T.T.H.; Le, T.Q.N.; Nguyen, N.H. Batch and column adsorption of reactive dyes by eggshell powder–chitosan gel core-shell material. *Mor. J. Chem.* **2021**, *9*, 18–27.
197. Noreen, S.; Bhatti, H.N.; Nausheen, S.; Sadaf, S.; Ashfaq, M. Batch and fixed bed adsorption study for the removal of Drimarine Black CL-B dye from aqueous solution using a lignocellulosic waste: A cost affective adsorbent. *Ind. Crops Prod.* **2013**, *50*, 568–579. [[CrossRef](#)]
198. Stavrinou, A.; Aggelopoulos, C.A.; Tsakiroglou, C.D. A Methodology to Estimate the Sorption Parameters from Batch and Column Tests: The Case Study of Methylene Blue Sorption onto Banana Peels. *Processes* **2020**, *8*, 1467. [[CrossRef](#)]
199. Dovi, E.; Aryee, A.A.; Kani, A.N.; Mpatani, F.M.; Li, J.; Qu, L.; Han, R. High-capacity amino-functionalized walnut shell for efficient removal of toxic hexavalent chromium ions in batch and column mode. *J. Environ. Chem. Eng.* **2022**, *10*, 107292. [[CrossRef](#)]
200. Vinodhini, V.; Das, N. Packed bed column studies on Cr (VI) removal from tannery wastewater by neem sawdust. *Desalination* **2010**, *264*, 9–14. [[CrossRef](#)]
201. Vilvanathan, S.; Shanthakumar, S. Modeling of fixed-bed column studies for removal of cobalt ions from aqueous solution using *Chrysanthemum indicum*. *Res. Chem. Intermed.* **2017**, *43*, 229–243. [[CrossRef](#)]
202. Vieira, M.L.G.; Martinez, M.S.; Santos, G.B.; Dotto, G.L.; Pinto, L.A.A. Azo dyes adsorption in fixed bed column packed with different deacetylation degrees chitosan coated glass beads. *J. Environ. Chem. Eng.* **2018**, *6*, 3233–3241. [[CrossRef](#)]
203. Basu, M.; Guha, A.K. Analysis of continuous bioadsorptive removal of cadmium in the light of circular economy and sustainability. *Bioresour. Technol. Rep.* **2022**, *18*, 101101. [[CrossRef](#)]
204. Abdolali, A.; Ngo, H.H.; Guo, W.; Zhou, J.L.; Zhang, J.; Liang, S.; Chang, S.W.; Nguyen, D.D.; Liu, Y. Application of a breakthrough biosorbent for removing heavy metals from synthetic and real wastewaters in a lab-scale continuous fixed-bed column. *Bioresour. Technol.* **2017**, *229*, 78–87. [[CrossRef](#)]
205. Basu, M.; Guha, A.K.; Ray, L. Adsorption of lead on lentil husk in fixed bed column bioreactor. *Bioresour. Technol.* **2019**, *283*, 86–95. [[CrossRef](#)] [[PubMed](#)]
206. Nithya, K.; Sathish, A.; Kumar, P.S. Packed bed column optimization and modeling studies for removal of chromium ions using chemically modified Lantana camara adsorbent. *J. Water Process. Eng.* **2020**, *33*, 101069. [[CrossRef](#)]
207. Sousa, F.W.; Oliveira, A.G.; Ribeiro, J.P.; Rosa, M.F.; Keukeleire, D.; Nascimento, R.F. Green coconut shells applied as adsorbent for removal of toxic metal ions using fixed-bed column technology. *J. Environ. Manag.* **2010**, *91*, 1634–1640. [[CrossRef](#)] [[PubMed](#)]
208. Sousa, F.W.; Sousa, M.J.; Oliveira, I.R.; Oliveira, A.G.; Cavalcante, R.M.; Fachine, P.B.; Neto, V.O.; de Keukeleire, D.; Nascimento, R.F. Evaluation of a low-cost adsorbent for removal of toxic metal ions from wastewater of an electroplating factory. *J. Environ. Manag.* **2009**, *90*, 3340–3344. [[CrossRef](#)] [[PubMed](#)]
209. Pereira, F.V.; Gurgel, L.V.; de Aquino, S.F.; Gil, L.F. Removal of Zn<sup>2+</sup> from electroplating wastewater using modified wood sawdust and sugarcane bagasse. *J. Environ. Eng.* **2009**, *135*, 341–350. [[CrossRef](#)]
210. Vijayaraghavan, K.; Palanivelu, K.; Velan, M. Crab shell-based biosorption technology for the treatment of nickel-bearing electroplating industrial effluents. *J. Hazard. Mater.* **2005**, *119*, 251–254. [[CrossRef](#)]
211. Zhou, G.; Luo, J.; Liu, C.; Chu, L.; Crittenden, J. Efficient heavy metal removal from industrial melting effluent using fixed-bed process based on porous hydrogel adsorbents. *Water Res.* **2018**, *131*, 246–254. [[CrossRef](#)]

212. Nunez-Gomez, D.; Rodrigues, C.; Lapolli, F.R.; Lobo-Recio, M.A. Adsorption of heavy metals from coal acid mine drainage by shrimp shell waste: Isotherm and continuous-flow studies. *J. Environ. Chem. Eng.* **2019**, *7*, 102787. [[CrossRef](#)]
213. Yahya, M.D.; Obayomi, K.S.; Orekoya, B.A.; Olugbenga, A.G.; Akoh, B. Process evaluation study on the removal of Ni (II) and Cu (II) ions from an industrial paint effluent using kola nut pod as an adsorbent. *J. Dispers. Sci. Technol.* **2021**, *43*, 105–113. [[CrossRef](#)]
214. Moreira, S.A.; Melo, D.Q.; de Lima, A.C.A.; Sousa, F.W.; Oliveira, A.G.; Oliveira, A.H.B.; Nascimento, R.F. Removal of Ni<sup>2+</sup>, Cu<sup>2+</sup>, Zn<sup>2+</sup>, Cd<sup>2+</sup> and Pb<sup>2+</sup> ions from aqueous solutions using cashew peduncle bagasse as an eco-friendly biosorbent. *Desalin. Water Treat.* **2016**, *57*, 10462–10475. [[CrossRef](#)]

**Disclaimer/Publisher's Note:** The statements, opinions and data contained in all publications are solely those of the individual author(s) and contributor(s) and not of MDPI and/or the editor(s). MDPI and/or the editor(s) disclaim responsibility for any injury to people or property resulting from any ideas, methods, instructions or products referred to in the content.